European Journal of Taxonomy 751: 115–139
https://doi.org/10.5852/ejt.2021.751.1383

ISSN 2118-9773
www.europeanjournaloftaxonomy.eu
2021 · Ballou L. *et al.*



**Research article**

urn:lsid:zoobank.org:pub:8F94BA1E-5A15-4897-ABFB-234FDBF2506B

# Monsters in the dark: systematics and biogeography of the stygobitic genus *Godzillius* (Crustacea: Remipedia) from the Lucayan Archipelago

Lauren BALLOU [1,*], Thomas M. ILIFFE [2], Brian KAKUK [3], Brett C. GONZALEZ [4], Karen J. OSBORN [5], Katrine WORSAAE [6], Kenneth MELAND [7], Kenneth BROAD [8], Heather BRACKEN-GRISSOM [9] & Jørgen OLESEN [10]

[1,2] Department of Marine Biology, Texas A&M University at Galveston, USA.
[2,3,8] Bahamas Caves Research Foundation, Marsh Harbor, Abaco Island, The Bahamas.
[2,4,5] Department of Invertebrate Zoology, National Museum of Natural History, Smithsonian Institution, Washington DC, USA.
[6] Department of Biology, University of Copenhagen, Denmark.
[7] Department of Biological Sciences, University of Bergen, Norway.
[8] Department of Environmental Science and Policy, Rosenstiel School of Marine and Atmospheric Science & Abess Center, University of Miami, USA.
[9] Institute of Environment and Department of Biology, Florida International University – Biscayne Bay Campus, USA.
[10] Natural History Museum of Denmark, University of Copenhagen, Denmark.

[*] Corresponding author: balloul@tamu.edu
[2] Email: iliffet@tamug.edu
[3] Email: bahamacave@aol.com
[4] Email: GonzalezB@si.edu
[5] Email: osbornk@si.edu
[6] Email: kworsaae@bio.ku.dk
[7] Email: Kenneth.Meland@uib.no
[8] Email: kbroad@rsmas.miami.edu
[9] Email: hbracken@fiu.edu
[10] Email: jolesen@snm.ku.dk

[1] urn:lsid:zoobank.org:author:C4E5D7A6-5783-4B13-9A0D-E23AD8D40654
[2] urn:lsid:zoobank.org:author:3F52E7D3-C2D4-4C5C-B62A-D28BC524B9B4
[3] urn:lsid:zoobank.org:author:19B69381-F005-44F8-BDBB-D1C5195E1693
[4] urn:lsid:zoobank.org:author:6BD1D9C0-2986-4A86-B3AF-33B117D092A0
[5] urn:lsid:zoobank.org:author:944106D7-E08A-4AB2-B904-E22F4DB156DE
[6] urn:lsid:zoobank.org:author:D5843EF7-2583-42D3-BB65-878E0E2EEF98
[7] urn:lsid:zoobank.org:author:F858E23C-6BC0-4E32-8372-CADD34E87D5A
[8] urn:lsid:zoobank.org:author:2E6CBB4A-D194-4D65-A2AE-F7F439C3C3EE
[9] urn:lsid:zoobank.org:author:81633725-4D97-453C-B85E-4CAEEF124C6A
[10] urn:lsid:zoobank.org:author:6B569425-6BE7-4A73-B165-87E0C097715A

**Abstract.** Remipedia is a stygobitic group commonly associated with coastal anchialine caves. This class consists of 12 genera, ten of which are found within the Lucayan Archipelago. Herein, we describe a new species within the genus *Godzillius* from Conch Sound Blue Hole, North Andros Island, Bahamas. *Godzillius louriei* sp. nov. is the third known remipede observed from a subseafloor marine cave, and the first from the Godzilliidae. Remipedes dwell within notoriously difficult to access cave habitats and thus integrative and comprehensive systematic studies at family or genus level are often absent in the literature. In this study, all species of *Godzillius* are compared using morphological and molecular approaches. Specifically, the feeding appendages of *G. louriei* sp. nov., *G. fuchsi* Gonzalez, Singpiel & Schlagner, 2013 and *G. robustus* Schram, Yager & Emerson, 1986 were examined using scanning electron microscopy (SEM). Species of *Godzillius* are identified based on the spines of maxilla 1 segment 4 and by the denticles on the lacinia mobilis of the left mandible. A molecular phylogeny using the mitochondrial 16S rRNA and nuclear histone 3 genes recovered *G. louriei* sp. nov. within the *Godzillius* clade and 16S genetic distances revealed a 13–15% difference between species of *Godzillius*.

**Keywords.** Anchialine, cave, new species, phylogeny.

Ballou L., Iliffe T.M., Kakuk B., Gonzalez B.C., Osborn K.J., Worsaae K., Meland K., Broad K., Bracken-Grissom H. & Olesen J. 2021. Monsters in the dark: systematics and biogeography of the stygobitic genus *Godzillius* (Crustacea: Remipedia) from the Lucayan Archipelago. *European Journal of Taxonomy* 751: 115–139. https://doi.org/10.5852/ejt.2021.751.1383

## Introduction

The crustacean class Remipedia is an enigmatic stygobitic group consisting of 29 species, 12 genera and eight families. Remipedes predominantly dwell within anchialine cave habitats (i.e., subterranean estuaries) (Bishop *et al.* 2015; Brankovits *et al*. 2017; van Hengstum *et al*. 2019). Like most anchialine fauna, remipedes exhibit a globally disjunct distribution, inhabiting submerged cave systems in the Caribbean, West Atlantic Ocean, Canary Islands and Western Australia (Koenemann & Iliffe 2014). A majority of remipedes (20 of 29 species) are reported from the Lucayan Archipelago (Bahamas and Turks and Caicos), suggesting a potential biodiversity hotspot for the group (Reid 1998). The karst dominated landscapes of these islands, as well as the presence of freshwater/saltwater mixing layers, provide optimal conditions for rapid dissolution and cave formation (Mylroie & Carew 1990; Mylroie & Mylroie 2011).

The clade Godzilliidae is one of four families endemic to the Lucayan Archipelago. Godzilliidae currently consists of two genera, *Godzilliognomus* Yager, 1989 and *Godzillius* Schram, Yager & Emerson, 1986. The family's name is attributed to the great size (43.2 mm) of the type species, *Godzillius robustus* Schram, Yager & Emerson, 1986, which is the largest observed remipede species to date (Schram *et al.* 1986). There are two previously described species within *Godzillius*: *G. robustus* and *G. fuchsi* Gonzalez, Singpiel & Schlagner, 2013. All members of *Godzillius* are found within the Lucayan Archipelago and are known to inhabit anchialine cave systems. *Godzillius robustus* occurs exclusively in Cottage Pond, North Caicos Island, Turks and Caicos Islands, while *G. fuchsi* inhabits the Dan's Cave and Ralph's Sink sections of the Dan's Cave System, Abaco Island, Bahamas (Fig. 1). Recent exploration of a subseafloor marine cave off Andros Island, Bahamas, revealed an unknown member of the genus *Godzillius*, described here.

Cryptic speciation can create taxonomic concerns for stygobitic fauna; thus, integration of morphological and molecular approaches (DNA barcoding) are useful in distinguishing species (Juan *et al.* 2010; Cánovas *et al.* 2016). Within Remipedia alone, *Xibalbanus fuchscockburni* (Neiber *et al.*, 2012), and *X. cozumelensis* Olesen *et al.*, 2017, were recognized as cryptic/pseudocryptic when compared to other members of their genus using mitochondrial genes (Neiber *et al*. 2012; Olesen *et al.* 2017). Since the use

of highly specialized technical cave diving technology is essential to access underwater cave systems, comprehensive comparisons across taxa are challenging and often absent from studies of Remipedia. Of the 29 previous remipede species descriptions, only four have included genetic data for species level identifications. Herein, we describe *Godzillius louriei* sp. nov. based on morphological (LM, SEM) and molecular techniques (16SrRNA and histone 3). Furthermore, we provide a morphological overview and molecular phylogenetic analysis of *Godzillius* with remarks on the biogeographic distribution of the genus.

## Material and methods

### Sampling and localities

A single remipede specimen (holotype) of *Godzillius louriei* sp. nov. was collected on 4 September 2017 in a 50 ml plastic Falcon tube from Conch Sound Blue Hole (25°07′ N, 78°00′ W), a subseafloor marine cave located 20–30 m offshore from North Andros Island, Bahamas. Conch Sound Blue Hole is the longest known subseafloor marine cave, consisting of a predominantly linear, southward trending conduit found just offshore from the northeastern coast of North Andros (Fig. 2) (Palmer 1997; Daenekas *et al*. 2009). The holotype was collected in the 'Collapse Room' at a water depth of 30–32 m and approximately 1600 m from the cave's only entrance. The remipede was collected in the saltwater

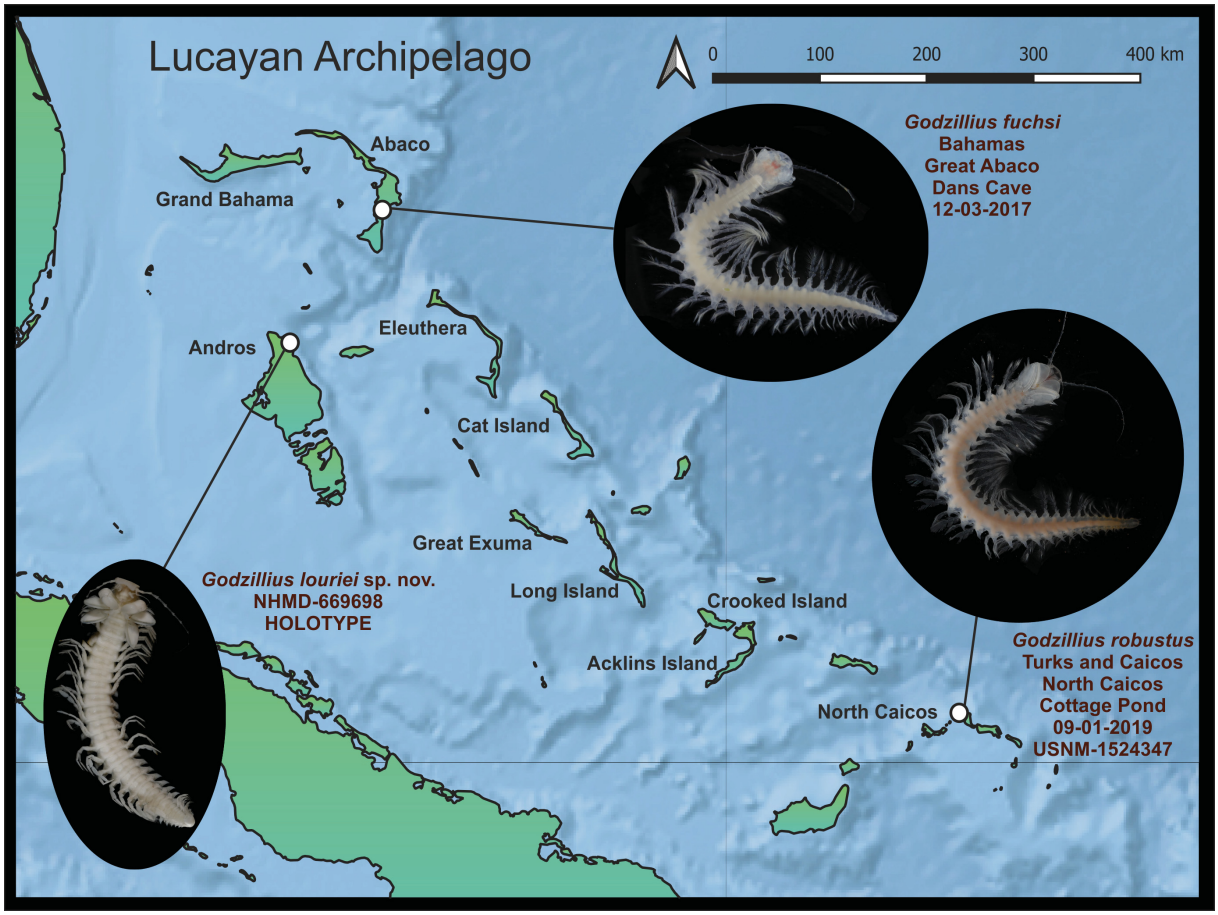


**Fig. 1.** Distribution of the genus *Godzillius* Schram, Yager & Emerson, 1986 within the Lucayan Archipelago. Type localities of *Godzillius fuchsi* Gonzalez, Singpiel & Schlagner, 2013, *G. louriei* sp. nov. and *G. robustus* Schram, Yager & Emerson, 1986 are indicated. Map constructed using the open source QGIS ver. 3.12 software (QGIS Development Team 2020) and metadata from Natural Earth (2020).

zone just above a hydrogen sulfide layer. The holotype was preserved in 80% ethanol and stored in the refrigerator prior to morphological and molecular work. Additional specimens used for comparative investigations were collected from Dan's Cave, Abaco Island, Bahamas in March 2017 (LB, TMI, BK, KM, JO) and in Cottage Pond, North Caicos Island, Turks and Caicos Islands (LB, TMI, BCG, KW, JO) in January 2019. Specimen details are provided below in 'Comparative material'.

### Photography, specimens and morphology

The single specimen of *G. louriei* sp. nov. was used for both morphological and molecular studies. Ten limbs were removed for molecular work (see below) prior to photographing the habitus of the specimen. All specimens were photographed using a Canon EOS 5D Mark IV fitted with a Canon Macro Twin Lite MT-24EX flash and a Canon MP-E 65mm f2.8 macro lens tethered to a PC and operated using standard EOS software. Depth of field in the final images of *G. louriei* sp. nov. was enhanced by shooting and combining z-stacks later blended using Zerene Stacker ver. 1.04. Left side mouthparts (maxilla 1, maxilla 2, maxilliped, both mandibles) and one trunk limb were removed and prepared for SEM. Additionally, the mouthparts (maxilla 1, maxilla 2, maxilliped) of two individuals of *G. fuchsi* and one individual of *G. robustus* were prepared for comparison. All dissected appendages for SEM were dehydrated in a graded ethanol series (80%, 90%, 95%, 100%), critical point dried, mounted on aluminum stubs and sputter coated with platinum/palladium. Morphological observations and micrographs were made using a JEOL JSM-6335-F (FE) field emission SEM at the Natural History Museum of Denmark (University of Copenhagen). Selected appendages (left antenna 1, left antenna 2, trunk limbs 1, 2, 7, 28 and 29) were additionally prepared on permanent slides. Slides were photographed using an inverted Olympus microscope (IX83) with automatized stacking and stitching capabilities. Terminology follows Gonzalez *et al.* (2013), Koenemann & Iliffe (2014) and Schram *et al*. (1986). Material of the new species is deposited at the Natural History Museum of Denmark (NHMD), University of Copenhagen.

### Comparative material

The following material of *Godzillius fuchsi* and *G. robustus* from NHMD and the National Museum of Natural History, Smithsonian Institution, Washington DC (USNM) were included for comparison:

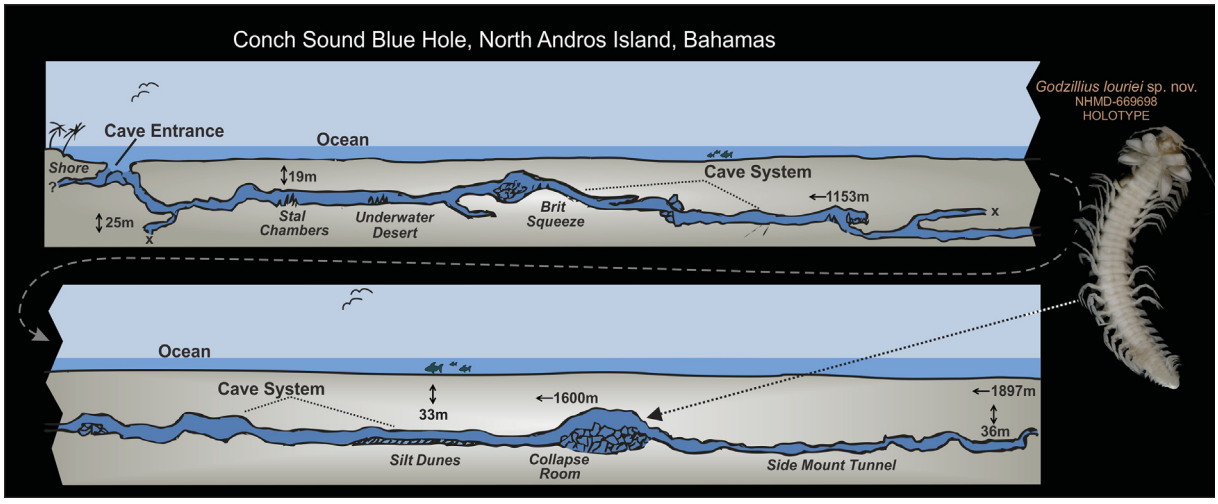


**Fig. 2.** Cave profile of Conch Sound Blue Hole, North Andros Island, the type locality of *Godzillius louriei* sp. nov. Sampling of *G. louriei* sp. nov. occurred in the "Collapse Room" at approximately 1600 m. Abbreviations: x = chambers too small for diver entry; ? = undescribed/unexplored passage; ← m = penetration distance from cave entrance; ↕ = depth of cave passage. Cave map illustrated by authors Brian Kakuk and Lauren Ballou; cave passages ranging from the entrance to 1153 m within the system were based off of previous illustrations and descriptions (Farr & Palmer 1984; Farr 2017).

*Godzillius fuchsi* Gonzalez, Singpiel & Schlagner, 2013
BAHAMAS • 4 specs; Abaco Island, Dan's Cave; 10 Mar. 2017; T. Iliffe and B. Kakuk leg.; GenBank: MW760694–MW760696, MW768707–MW768709; NHMD 165814, 165841, 165850, 165860.

*Godzillius robustus* Schram, Yager & Emerson, 1986
TURKS AND CAICOS ISLANDS • 2 specs; North Caicos, Cottage Pond; 9 Jan. 2019; T. Iliffe and P. Heinerth leg.; GenBank: MW760697–MW760698, MW768710–MW768711; USNM 1524345, 1524349.

**Taxon selection for molecular phylogeny**

In order to systematically evaluate our new material, we compared it with all other species within *Godzillius* and *Godzilliognomus* (Table 1). A total of six individuals across three species were newly sequenced: three *Godzillius fuchsi*, two *G. robustus* and one *G. louriei* sp. nov. Additionally, eight individuals across four species were obtained from GenBank (Benson *et al*. 1998) for this study: one *G. robustus*, two *Godzilliognomus schrami* Iliffe, Otten & Koenemann, 2010, four *Godzilliognomus frondosus* Yager, 1989 and one *Cryptocorynetes haptodiscus* Yager, 1987. *Cryptocorynetes haptodiscus* (Cryptocorynetidae) was selected as the outgroup as it was shown to be one of the closest relatives to Godzilliidae that has data available in GenBank (Hoenemann *et al*. 2013).

**DNA extraction, amplification, sequencing, molecular analyses**

Trunk limb tissue was dissected from our new material, three individuals of *G. fuchsi* and two individuals of *G. robustus*. DNA extraction was performed using the Qiagen DNeasy Tissue and Blood Kit following the manufacturer's protocol. 16S rRNA and histone 3 (H3) were selected for amplification by polymerase chain reaction (PCR) using primers sets 16S arL/brH (5′ CGCCTGTTTATCAAAAACAT 3′) (5′ CCGGTCTGAACTCAGATCACGT 3′) and H3 AF/AR (5′ ATGGCTCGTACCAAGCAGACVGC 3′) (5′ ATATCCTTRGGCATRATRGTGAC 3′) with M-13 F/R tails, respectively (Colgan *et al*. 1998; Palumbi *et al.* 2002). While mitochondrial genes are typically selected for species level differentiation, the nuclear gene H3 was also selected, as significant variation can be observed at the species level within Remipedia (Hoenemann *et al*. 2013). PCR reaction mixtures totaled 25 µl and included GoTaq polymerase (12.5 µl), forward and reverse primers (1 µl each), RNAfree water (8.5 µl) and DNA template (2 µl). All PCR reactions began using the following temperature profiles: denaturation at 94°C for 3:30 min; 35–40 annealing cycles, 30 seconds each between 40–50°C for 16S and 50°C for H3; an extension period at 72°C for 1:00 min; and a final extension at 72°C for 7:00 min. PCR reactions were visualized on 1–2% agarose gels stained with GelRed. Successful PCR productions (20 µl) were sent to GENEWIZ (South Plainfield, NJ) for sequencing.

Sequences (16S rRNA and H3) of *G. louriei* sp. nov. (n = 2), *G. fuchsi* (n = 6) and *G. robustus* (n = 4) were visually inspected, trimmed and cleaned using Geneious Prime ver. 2019.2.3 (Kearse *et al*. 2012). All sequences were checked for potential contamination by running a nucleotide BLAST similarity search (Altschul *et al*. 1990). Protein-coding H3 gene sequences were inspected for stop codons and point mutations using Geneious Prime to reduce the risk of including pseudogenes (Song *et al*. 2008). All sequence data were submitted to GenBank under accession numbers MW760694–MW760699 and MW768707–MW768712. The GenBank H3 gene sequence of *G. robustus* (KC989960) was excluded due to probable contamination, as the sequence genetically resembled that of *Godzilliognomus*. Sequences from multiple individuals previously identified as *Godzilliognomus schrami* and *Godzilliognomus frondosus* were concatenated from available GenBank data for H3 and 16S rRNA sequences to avoid excessive gaps in the phylogeny. These included KC989961+KC989998, KC989983+KC989999 and KC989962+KC990013. As these sequences were not from the same individuals, individual gene trees for H3 and 16S rRNA were constructed using maximum likelihood to identify potential issues from concatenation, and are provided in the supplementary material (Supplementary File 1 and Supplementary File 2).

**Table 1.** Taxon and voucher information for all sequence data included in phylogenetic and pairwise distance analyses. GenBank accession numbers provided for each gene used; bolded individuals indicate sequence data novel to this study (HBG = Florida International University Crustacean Collection).

| Taxon | Voucher | 16S | H3 | Included in Phylogeny | Included in Pairwise Distance |
|---|---|---|---|---|---|
| *Angirasu benjamini* | 06_047_2 | KC990007 | | | x |
| *Angirasu benjamini* | AB06_SS3 | KC990011 | | | x |
| *Angirasu benjamini* | AB06_TM1 | KC990012 | | | x |
| *Angirasu parabenjamini* | 04_023_SK | KC990017 | | | x |
| *Cryptocorynetes elmorei* | 07_035B | KC989996 | | | x |
| *Cryptocorynetes haptodiscus* | AB06_SS1_1 | KC989997 | KC989967 | x | x |
| *Godzilliognomus frondosus* | 06_048_4 | KC989998 | | x | x |
| *Godzilliognomus frondosus* | AB06_SS_4.1 | KC989999 | | x | x |
| *Godzilliognomus frondosus* | 06_50_3 | | KC989983 | x | |
| *Godzilliognomus frondosus* | Gn_06_47_8 | | KC989961 | x | |
| *Godzilliognomus schrami* | 07_048_2 | KC990013 | | x | x |
| *Godzilliognomus schrami* | 07_49 | | KC989962 | x | |
| ***Godzillius fuchsi*** | **NHMD-165814; HBG 9565** | **MW768707** | **MW760694** | **x** | **x** |
| ***Godzillius fuchsi*** | **NHMD-165860; HBG 9600** | **MW768709** | **MW760696** | **x** | **x** |
| ***Godzillius fuchsi*** | **NHMD-165850; HBG 9595** | **MW768708** | **MW760695** | **x** | **x** |
| ***Godzillius louriei* sp. nov.** | **NHMD-669698; HBG 9820** | **MW768712** | **MW760699** | **x** | **x** |
| ***Godzillius robustus*** | **USNM-1524349, HBG 9727** | **MW768710** | **MW760697** | **x** | **x** |
| ***Godzillius robustus*** | **USNM-1524345, HBG 9733** | **MW768711** | **MW760698** | **x** | **x** |
| *Godzillius robustus* | 03_19 | KC990000 | | x | x |
| *Kumonga exleyi* | BES-10169 | KC990002 | | | x |
| *Lasionectes entrichoma* | 03_16 | KC990001 | | | x |
| *Micropacter yagerae* | 41698 | KC990003 | | | x |
| *Morlockia atlantida* | DZUL_9999_GBIF | FJ905031 | | | x |
| *Morlockia atlantida* | LZ_1_1 | FJ905032 | | | x |
| *Morlockia atlantida* | LZ_2_1 | FJ905033 | | | x |
| *Morlockia atlantida* | LZ_2_3 | FJ905034 | | | x |
| *Morlockia emersoni* | 05_022_1 | KC990008 | | | x |
| *Morlockia ondinae* | LZ_1_2 | FJ905035 | | | x |
| *Morlockia williamsi* | 08_033_4 | KC990018 | | | x |
| *Pleomothra apletocheles* | AB06_RS2 | KC990004 | | | x |
| *Pleomothra apletocheles* | AB06_SS2 | KC990005 | | | x |
| *Pleomothra apletocheles* | | GU067680 | | | x |
| *Pleomothra* sp. nov. | 07_038 | KC990014 | | | x |
| *Speleonectes gironensis* | | AF370874 | | | x |
| *Speleonectes kakuki* | BH330 | KC990009 | | | x |
| *Speleonectes lucayensis* | AB06_LR_1 | KC990010 | | | x |
| *Speleonectes* sp. nov. | AB06_047_6 | KC990015 | | | x |
| *Speleonectes* sp. nov. | AB06_DC_1.1 | KC990016 | | | x |
| *Xibalbanus cozumelensis* | ZMUC_CRU_4793 | KX830886 | | | x |
| *Xibalbanus cf tulumensis* | 06_041H | KC990019 | | | x |
| *Xibalbanus tulumensis* | | AY456190 | | | x |

Sequences were aligned using the MAFFT ver. 7 auto-iterative alignment program (Katoh *et al.* 2019). MAFFT was selected due to its greater accuracy relative to other alignment programs (Pais *et al*. 2014). Gene alignments were subsequently concatenated within Geneious Prime (H3: 327bp, 16S: 543bp). Both Maximum Likelihood (ML) and Bayesian Inference (BI) were utilized. ML substitution models for each gene were selected based on the Akaike Information Criterion (AIC) in ModelFinder within IQ-Tree ver. 1.6.11 (Nguyen *et al.* 2014; Kalyaanamoorthy *et al*. 2017). The most optimal DNA substitution models for ML analyses of 16S rRNA and H3 alignments were GTR + F + R2 and TN + F + G4, respectively. The optimal AIC model for BI analyses of both 16S rRNA and H3 alignments was GTR + G. Individual gene trees and the concatenated gene tree were constructed using the program IQ-TREE for Maximum Likelihood (ML) analyses (Nguyen *et al.* 2014). IQ-TREE was selected for this analysis as it was shown to outperform other ML programs in increased likelihood values when analyzing concatenated species trees (Zhou *et al*. 2017). Nodal support was quantified using ultrafast bootstrapping methods (UFBoot) with 1000 replicates (Hoang *et al.* 2018). jModelTest ver. 2.1.10 (Guindon & Gascuel 2003; Darriba *et al*. 2012) was used to find the optimal BI substitution models based on AIC and the alignment was subsequently run in MrBayes ver. 3.2.6 (Ronquist *et al*. 2012) on XSEDE within the Cipres Science Gateway (Miller *et al*. 2010). Four Markov Chain Monte Carlo (MCMC) chains were run twice for 30 000 000 generations with a burn-in of 10 000 000. Convergence was evaluated using trace plots and effective sample size (ESS > 200) within the program Tracer ver. 1.7.1 (Rambaut *et al.* 2018).

Molecular variation in *Godzillius* relative to that in other genera within Remipedia was compared using 16S rRNA sequence pairwise distances calculated using p-distance and pairwise deletion of gaps in MEGA ver. 7 (Kumar *et al*. 2016). All GenBank 16S rRNA material was used, with the exception of a potentially contaminated sequence of *Pleomothra apletocheles* Yager, 1989 KC990006 (Table 1).

**Abbreviations**

a1 = antenna 1
a2 = antenna 2
md = mandible
mx1 = maxilla 1
mx2 = maxilla 2
mxp = maxilliped

## Results

### *Systematics*

Subphylum Crustacea Brünnich, 1772
Class Remipedia Yager, 1981
Order Nectiopoda Schram, 1986
Family Godzilliidae Schram, Yager & Emerson, 1986
Genus *Godzillius* Schram, Yager & Emerson, 1986

***Godzillius louriei*** Ballou, Bracken-Grissom & Olesen sp. nov.
urn:lsid:zoobank.org:act:F0D0FD57-4ACF-4BC3-B8D2-CBCF00E16026
Figs 3–8

**Diagnosis**

25 mm in length with 29 trunk segments. Cephalic shield subtrapezoidal. Pleurotergite lateral margins pointed posteriorly. Sternal bars isomorphic. A1 bifurcated, dorsal branch with 11 articles. Right and left md gnathal edges crescentiform, asymmetrical; left lacinia mobilis with 5 denticulae. Mx1 with

7 segments; segment 1 with 10 large and 3 small spines; segment 4 endite digitiform, anterior margin lined with 10 conical denticulae. Mx2 with 6 segments; distal segment unguiform, bearing seven denticulae. Mxp with 9 segments; terminal claw with conical, laminate spines. Caudal rami short and distally covered with plumose setae.

**Etymology**

Named for Robert Lourie whose financial support of the Bahamas Caves Research Foundation contributes to furthering cave and blue hole related research in the Bahamas. The taxonomic description and underlying molecular justification for *Godzillius louriei* sp. nov. was prepared by LB, HBG, and JO, who are thus responsible for making the specific name *louriei* available.

**Material examined**

**Holotype**

BAHAMAS • holotype; North Andros Island, Conch Sound Blue Hole, The Collapse Room; 25°07′ N, 78°00′ W; depth 30–32 m, approximately 1600 m horizontal distance from single cave entrance; 4 Sep. 2017; B. Kakuk leg.; specimen dissected and distributed on four light microscopy slides, six SEM stubs and one alcohol voucher; GenBank: MW760699, MW768712; NHMD 669698.

**Description**

Cephalon (Fig. 3). Cephalic shield subtrapezoidal, posterior margins wider than anterior. Posteriolateral margins rounded; sutures absent. Anterior margin folds ventrally, covering a1 aesthetascs and bifurcated frontal filaments.

Body (Fig. 3). Body length 25 mm; 29 trunk segments. Pleurotergite lateral margins pointed posteriorly. Sternal bars isomorphic. Trunk limbs bifurcated with endopods and exopods consisting of three and four segments respectively. Trunk limbs 1 and 18–29 reduced in size (Figs 3–4). Trunk limb 14 protopod with large lobate protrusion and ventrally with slender genital flap (Fig. 3F).

Antenna 1 (Fig. 4A). Biramous, located posterior to frontal filaments. Peduncle with two articles; proximal article bearing numerous aesthetascs. Distal peduncle article bifurcated, acts as base of dorsal and ventral rami. Dorsal ramus (i.e., dorsal branch) with 11 articles; girth decreasing distally through articles. Article 1 with single anteriodistal setal cluster; article 2 with one medial seta, one distal cluster; article 3 with two medial setae; article 4 with two medial setae, one distal seta, fine marginal setae; article 5 with one medial seta, one distal cluster; article 6 with three medial setae, one distal seta; article 7 possessing two to three medial setae, one distal seta; article 8 bearing one fine medial seta; articles 9 and 10 lacking setae; article 11 with terminal tuft of setae. Ventral ramus (i.e., ventral branch) with ambiguous articulation, treated as three articles (Fig. 4A). Proximal article shorter than article 2, no setae, partly fused with peduncle. Article 2 length ~2× that of proximal article. Article 3 length ~3× that of article 2, with one filiform medial seta and a distal setal tuft.

Antenna 2 (Fig. 4B). Protopod with two articles (i.e., coxa and basis). Basis with exopod unarticulate and endopod of three articles. Exopod ovoid, lateral margin with ~50 long, plumose setae. Endopod proximal article distomedial margin bearing two long setae. Article 2 median margin with 10–20 long setae; lateral margin with 3–4 short setae. Article 3 entire margin with 55–65 setae.

Mandible (Fig. 5). Gnathal edge comprised of lacinia mobilis, incisor and molar process. Molar processes crescentiform, with slight invagination along midline. Molar process wider ventrally than dorsally, covered in setae. Left and right md asymmetrical; right incisor with three slightly serrated denticulae extending medially towards atrium oris; left with three distinctly serrated denticulae and small fourth tooth on posterior margin. Right lacinia mobilis with three slightly serrated denticulae; left with five smooth, uneven denticulae.

Maxilla 1 (Fig. 6). Comprised of seven segments, posterior to a2. Segment 1 with medially-extending endite bearing ten conical spines and three small spines (Fig. 6D–E). Segment 2 with dorso-ventrally flattened, broad, spatulate endite; oblong distal edge of endite with 4–5 short conical spines and 25–30 moderate to long simple setae. Segment 3 with no setae nor endites. Segment 4 robust with single digitiform endite extending medially; medial anterior margin bearing ten conical denticles, decreasing in

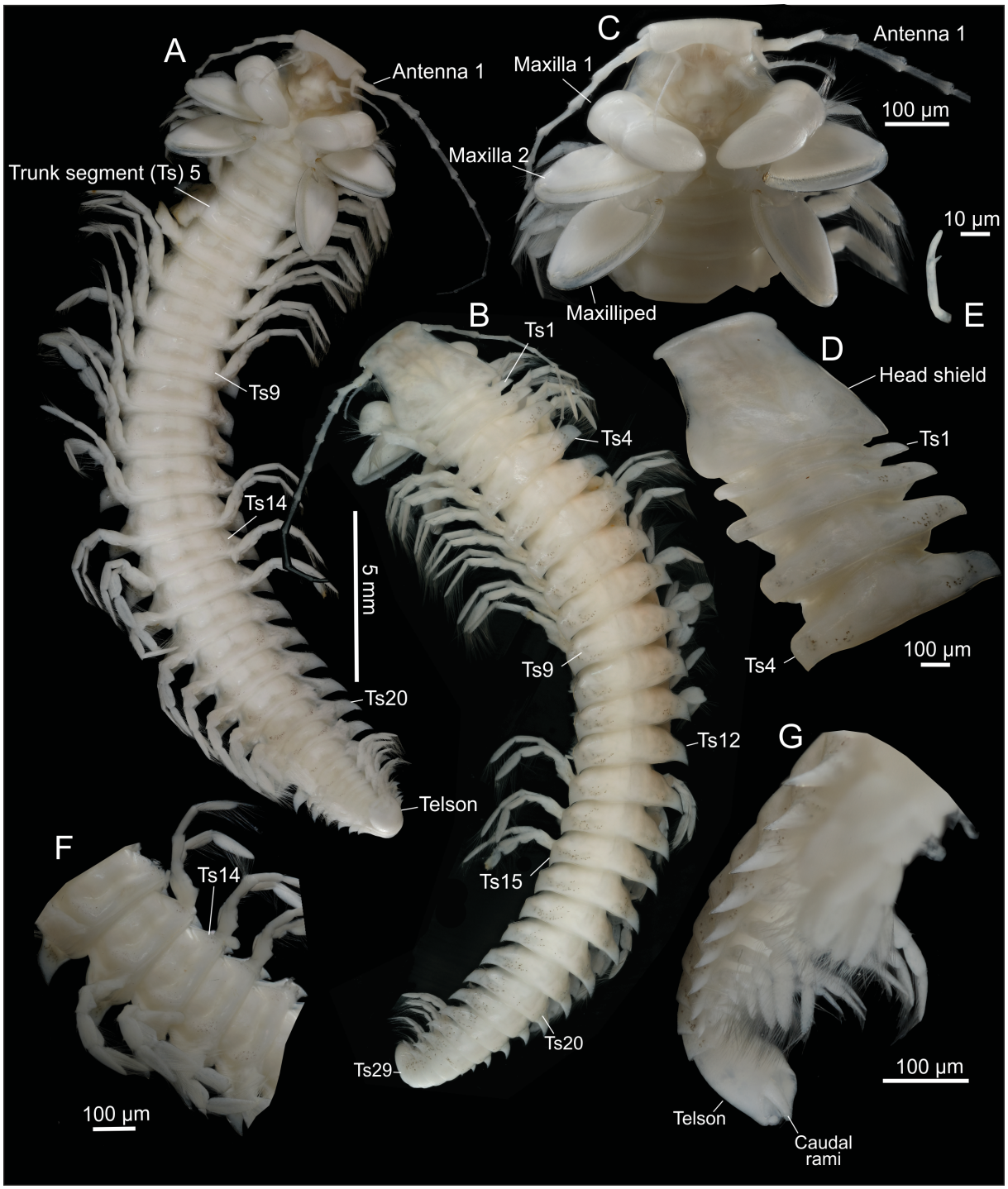


**Fig. 3.** *Godzillius louriei* sp. nov., holotype (NHMD 669698), light microscopy. **A**. Entire animal, ventral view. **B**. Entire animal, dorsal view. **C**. Cephalon, ventral view. **D**. Cephalon, dorsal view. **E**. Frontal filament, left side. **F**. Sternal bars and trunk segments (Ts), ventral view. **G**. Telson, lateral view.

size distally, and endite disto-medial edge with ~19–20 long, simple setae (Fig. 6F). Segment 4 antero-medial face with setal cluster of 11 moderate, simple setae. Segment 5 robust, with proximal cluster of simple setae. Segment 6 narrow, ventral margin with a long, simple setal cluster (at least 23 setae); anterior and posterior faces with two long, simple clusters. Segment 7 with long, simple setal cluster

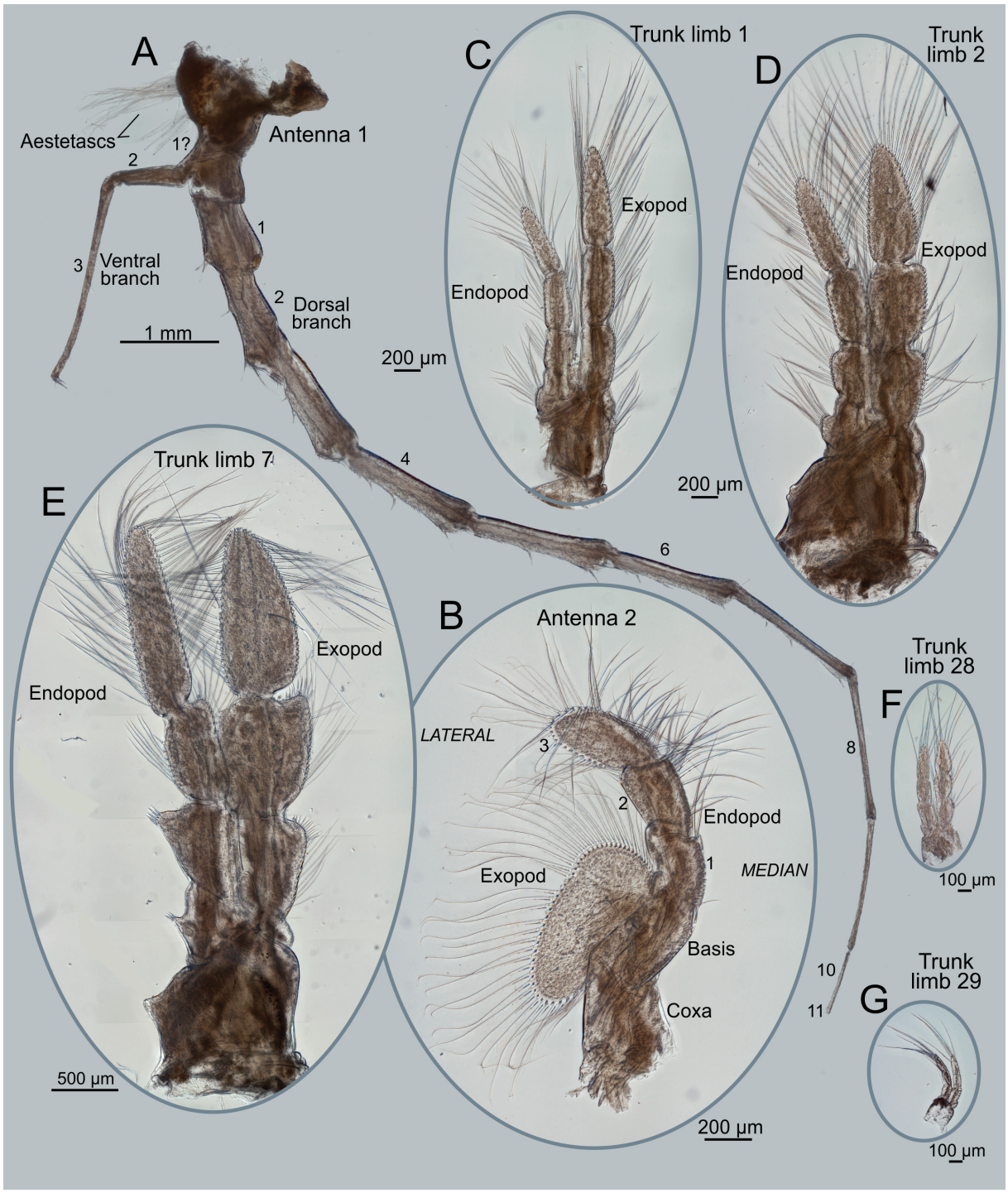


**Fig. 4.** *Godzillius louriei* sp. nov., holotype (NHMD 669698), light microscopy. **A**. Antenna 1 (a1), dorsal view. **B**. Antenna 2 (a2), dorsal view. **C**. Trunk limb 1. **D**. Trunk limb 2. **E**. Trunk limb 7. **F**. Trunk limb 28. **G**. Trunk limb 29. Small numbers represent segments of the dorsal and ventral branches of a1 and the exopod of a2.

underneath elongate, robust, talon-like claw. Claw distally curved towards atrium oris; duct opening at distal tip.

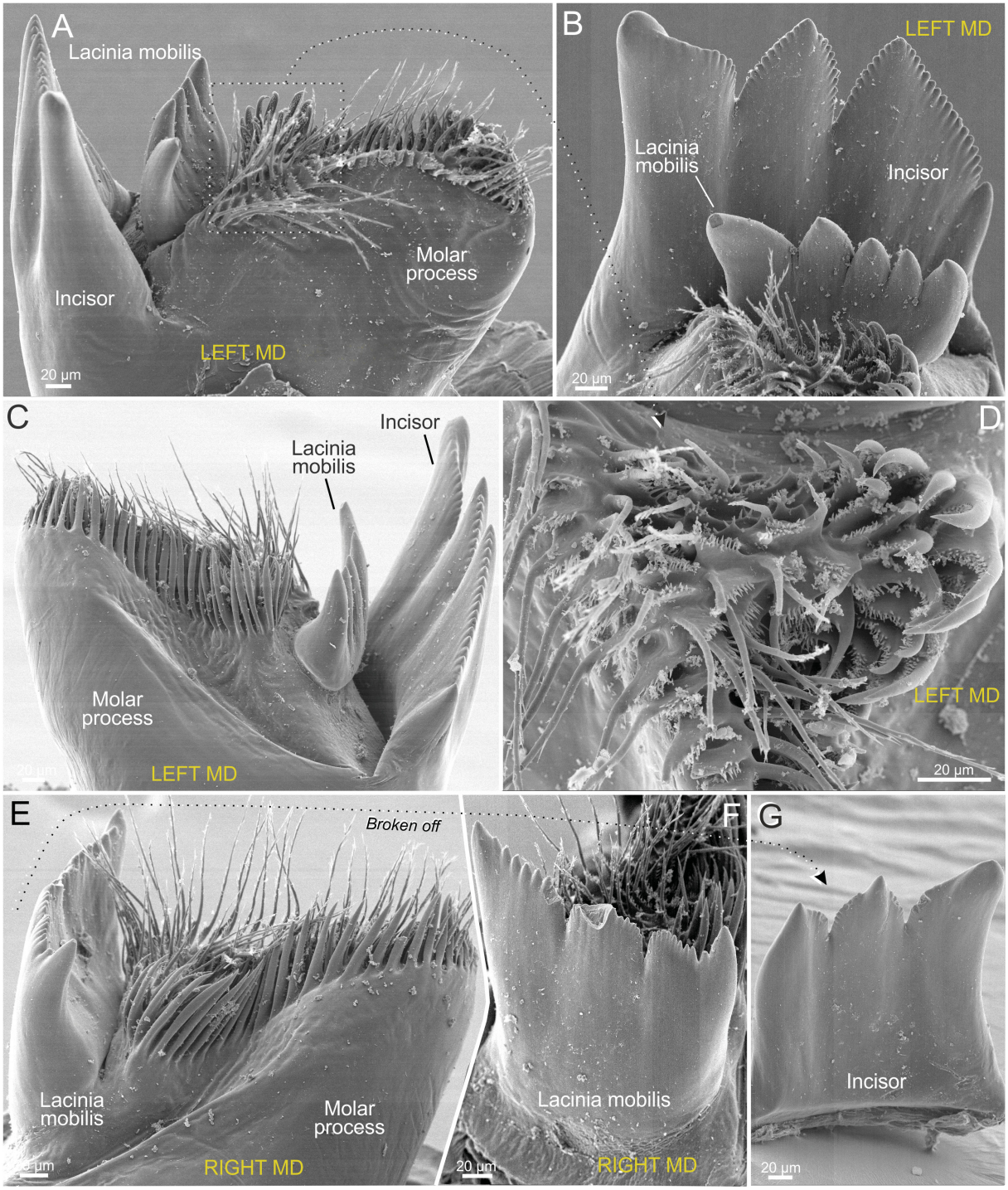


**Fig. 5.** *Godzillius louriei* sp. nov., holotype (NHMD 669698), scanning electron microscopy. **A**. Left mandible (md), anterior view. **B**. Left md, apical view of the lacinia mobilis and incisor. **C**. Left md, posterior view. **D**. Left md, apical view of the setae within the molar process. **E**. Right md, posterior view; incisor unintentionally removed in dissection. **F**. Right md, ventral view of the gnathal edge without the incisor. **G**. Right md, ventral view of the incisor.

Maxilla 2 (Fig. 7). Comprised of six segments, posterior to mx1. Segment 1 with three digitiform endites (a–c on Fig. 7K–L) angled antero-medially; each endite distal margin with one conical spine, pore cluster and a variable number of short, simple setae (endite a, 5 setae; endite b, 14; endite c, 15). Each endite anterior margin with long, simple setae (endite a, 1 seta; endite b, 2; endite c, 2). Segment 1 posterior maxillary gland comprised of large tubular conduit opening toward cephalic shield (Fig. 7J). Segment 2 with one conical endite extending postero-medially; bearing distal cluster of short, simple setae (Fig. 7G–I). Segment 3 (lacertus) somewhat triangular, longer than segments 1 and 2 combined. Lacertus ventral margin extending beyond dorsal margin; with ~four rows of moderate-to-long, vertically striated setae. Brachium (segments 4–6) extending length of lacertus; terminal claw spines extend beyond lacertus. Segment 4 extending ~$^{4}/_{5}$ length of brachium; fine setae throughout segment, with 1–3 short, simple setae at ventral distal end. Segment 5 $^{1}/_{5}$ length of brachium; distal margins with four short, simple setal clusters (5–6 setae in each). Segment 6 with distal arrangement of seven conical spines decreasing in length distally; curved downward over setal pad in a grappling hook arrangement (terminal claw complex) (Fig. 7D–F). Setal pad with long, simple setae; proximal edge conical, lacking setae, directed towards lacertus.

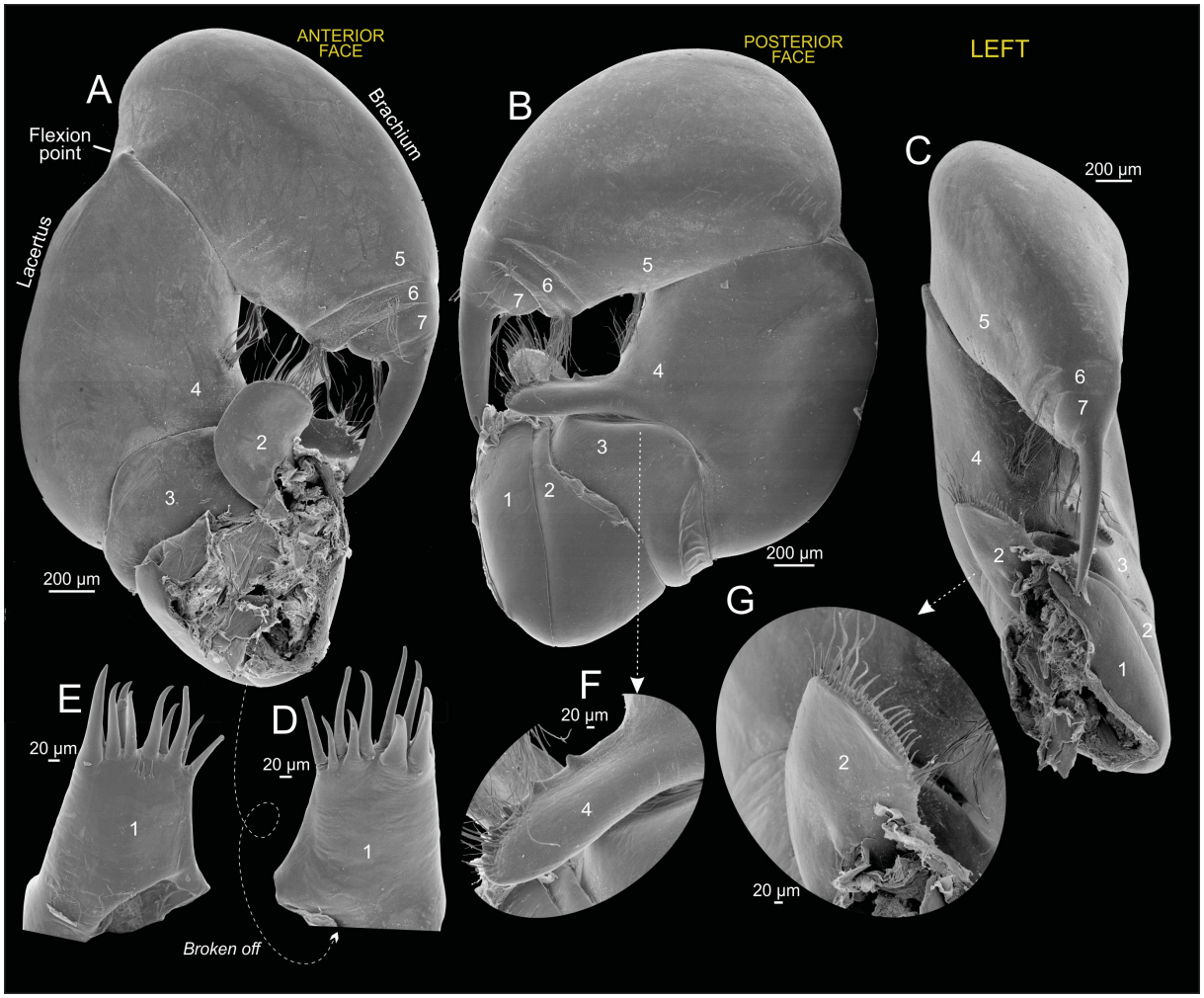


**Fig. 6.** *Godzillius louriei* sp. nov., holotype (NHMD 669698), left maxilla 1 (mx1), scanning electron microscopy. **A**. Anterior face of mx1. **B**. Posterior face of mx1. **C**. Apical view of mx1. **D**–**E**. Endite of segment 1, unintentionally removed during dissection. **F**. Conical spines along the surface of the digitiform endite on segment 4, posterior view. **G**. Spatulate endite of segment 2, apical view. Small numbers represent segments of mx1.

Maxilliped (Fig. 8). Comprised of nine distinct segments, with flexion point between segments 5 and 6. Segment 1 with one medial setal cluster of five small, vertically striated setae. Segment 2 anterior face proximal medial margin with eight vertically striated setae; posterior face medial margin with six short, vertically striated setae. Segment 3 triangular along posterior face; proximal margin three times wider than distal margin. Distal margin of segments 3 and 4 align, reaching proximal margin of segment 5


**Fig. 7.** *Godzillius louriei* sp. nov., holotype (NHMD 669698), left maxilla 2 (mx2), scanning electron microscopy. **A**. Anterior face of mx2; endites of segment 1 indicated as lowercase letters a–c. **B**. Apical view of mx2. **C**. Posterior face of mx2. **D**. Terminal claw, apical view. **E**. Terminal claw, posterior face. **F**. Terminal claw, anterior face. **G**. Endite of segment 2, median view. **H**. Endite of segment 2, posterior face. **I**. Hollowed conical tip of the endite of segment 2. **J**. Maxillary gland opening of mx2. **K**. Triplet endites of segment 1 (a–c) and singular endite of segment 2, posterior face. **L**. Triplet endites of segment 1 (a–c) and singular endite of segment 2, apical view. **M**. Conical spine on the third endite of segment 1, apical view. **N**. Conical spine on the second endite of segment 1, apical view. **O**. Conical spine on the first endite of segment 1, apical view. Small numbers represent segments of mx2.

(lacertus). Segment 3 anterior face rectangular and narrower than segment 2; proximal medial margin bearing four small setae (2 grooved, 1 simple, 1 conical). Segment 4 exhibiting different shapes along anterior and posterior faces. Segment 4 posterior face triangular, with proximal margin narrower than distal margin; proximal margin with one vertically-striated seta and 2–3 simple setae. Segment 4 anterior face rectangular, small suture along its length; with two small, vertically striated setae. Segment 5 similar

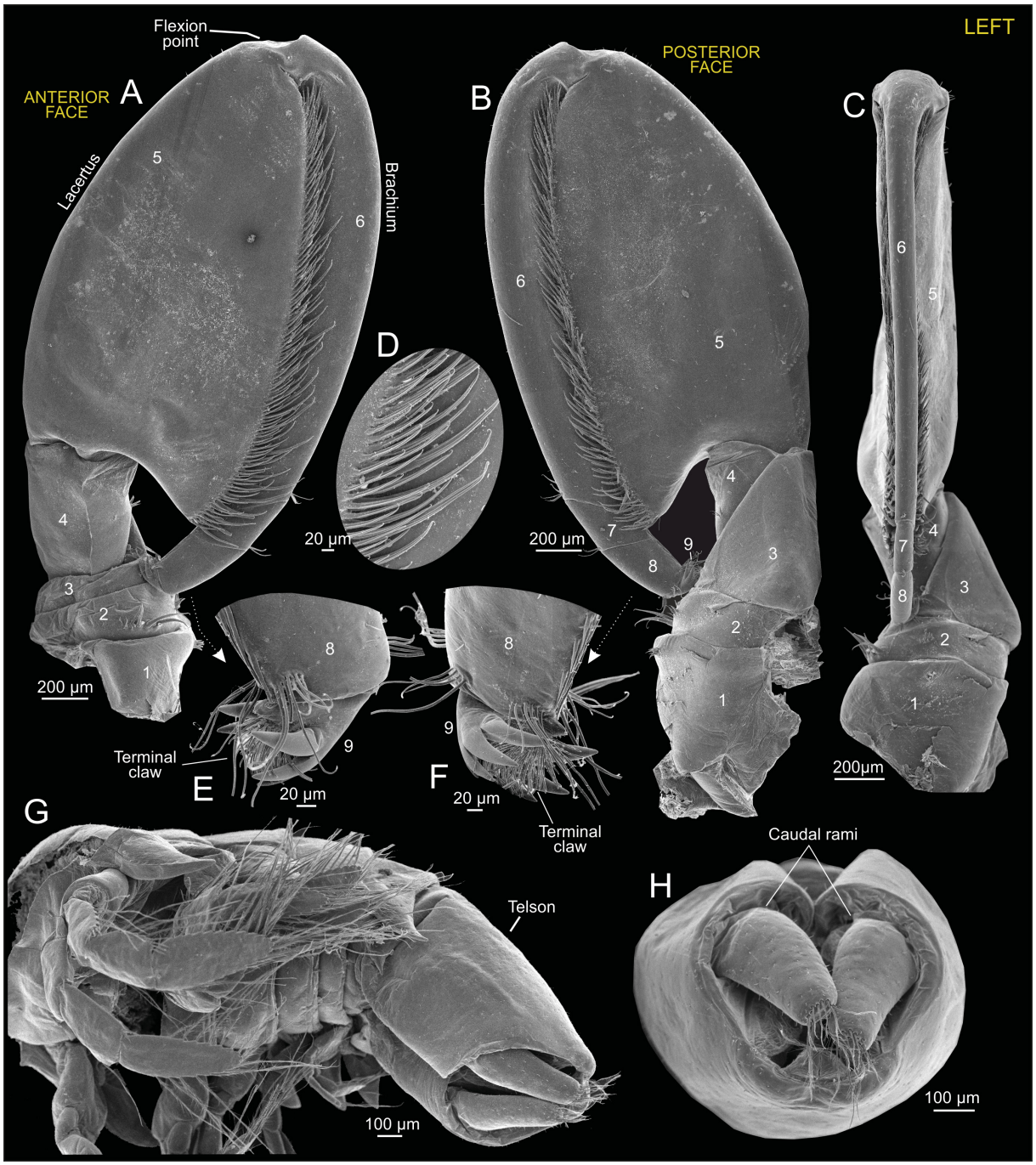


**Fig. 8.** *Godzillius louriei* sp. nov., holotype (NHMD 669698), left maxilliped (mxp) scanning electron microscopy. **A**. Anterior face of mxp. **B**. Posterior face of mxp. **C**. Apical view of mxp. **D**. Vertical striations of setae along the surface of the lacertus. **E**. Terminal claw, anterior face. **F**. Terminal claw, posterior face. **G**. Posterior segments and telson, ventral view. **H**. Telson, lateral view; caudal rami separated by invagination of the telson. Small numbers represent segments of mxp.

in shape to lacertus of mx2; width decreasing proximally to distally. Lacertus with rows of vertically striated setae along ventral margin (Fig. 8D). Segments 6–9 (brachium) extending beyond length of lacertus. Brachium with short setae along surface, subsiding at terminal claw complex. Segment 6 nearing length of lacertus; distal margin with setal cluster of three simple setae. Segment 7 ~1/8 length of segment 6; extends beyond lacertus with distal cluster of three simple setae. Segment 8 longer than segment 7, with one setal cluster (5 simple setae, moderate length) above terminal claw, one posterior cluster (5 simple setae, moderate length) and two clusters (several simple setae, moderate length) oriented towards lacertus. Segment 9 with terminal claw complex (Fig. 8E–F); at least seven curved spines extending over setal pad (difficult to give exact number due to position of appendage). Six most proximal spines conical, robust; distal spine(s) small, laminate. Setal pad covered by terminal claw, protrudes downward, with long simple setae.

Telson, caudal rami (Figs 3, 8). Telson subrectangular, slightly longer than wide; ventral surface medial axis with deep invagination. Caudal rami short, extending distally past edge of telson; surface bearing short, scattered, simple setae. Each ramus distal margin with single cluster of ~10 long, plumose setae.

**Remarks**

Species of *Godzillius* can be distinguished by several morphological characters, most notably relating to the md and the three pairs of prehensile/raptorial post-mandibular mouthparts (Figs 9–10, Table 2). On the left md, the lacinia mobilis of both *G. louriei* sp. nov. and *G. fuchsi* have five denticulae, whereas *G. robustus* has six. One of the most striking distinctions between species of *Godzillius* is the number of conical denticles on the mx1 endite segment 4 anteriodistal margin (Fig. 9B, F, J). While *G. fuchsi* and *G. robustus* have been observed or described as having between 6 and 8 denticles along its margin, *G. louriei* sp. nov. has 10. Furthermore, the mx1 endite first segment has a unique spination, with 10 large spines and 3 small (Fig. 9D), contrasting with those of *G. robustus* (11 large, 4 small) and *G. fuchsi* (10 large, 2 small).

The terminal claw of mx2 in *G. robustus* is reported to have 10 free spines, whereas that of *G. fuchsi* and *G. louriei* sp. nov. have 7 (Fig. 9O, R, U). The mxp terminal claw in *G. fuchsi* has an elongate protrusion of the setal pad that is not covered by its spines (Fig. 10F); in contrast, the spines of *G. louriei* sp. nov. and *G. robustus* cover the setal pad (Fig. 10B, D). The mxp terminal claw of *G. robustus* has been described as a "grappling hook" with ten spines wrapping around a setal pad (Schram *et al.* 1986). *Godzillius louriei* sp. nov. has a similar arrangement, with at least 7 spines in the grappling hook arrangement (Fig. 10B). *Godzillius fuchsi* differs from the aforementioned species, having shorter, denticle-like spines with narrow spaces between them and not covering a distinctly protruding setal pad (Fig. 10F). We found the mxp of all three species to be composed of 9 segments (Fig. 10), modifying the previous descriptions of *G. robustus* and *G. fuchsi*, where fewer proximal segments were identified. It should be noted that this number of mxp segments coincides with what is reported for all other remipede species (Koenemann & Iliffe 2014).

## *Key to* Godzillius

1. Mx1 segment 4 without digitiform endite .....***Godzilliognomus*** Yager, 1989
– Mx1 segment 4 with digitiform endite .....2

2. Mx1 endite segment 4 with ten conical denticulae .....***Godzillius louriei*** sp. nov.
– Mx1 endite segment 4 with six to eight conical denticulae .....3

3. Left md lacinia mobilis with five denticulae .....
.....***Godzillius fuchsi*** Gonzalez, Singpiel & Schlagner, 2013
– Left md lacinia mobilis with six denticulae ...***Godzillius robustus*** Schram, Yager & Emerson, 1986

### *Phylogeny and pairwise distances*

The same topology was recovered in both Bayesian and maximum likelihood analyses of the concatenated dataset (Fig. 11). Within the Godzilliidae, two clades were recovered with full support across analyses (UFBoot = 100, BPP = 1.0), corresponding to the genera *Godzilliognomus* and *Godzillius*. *Godzilliognomus* formed a fully supported clade, and included the species *G. frondosus* and *G. schrami*

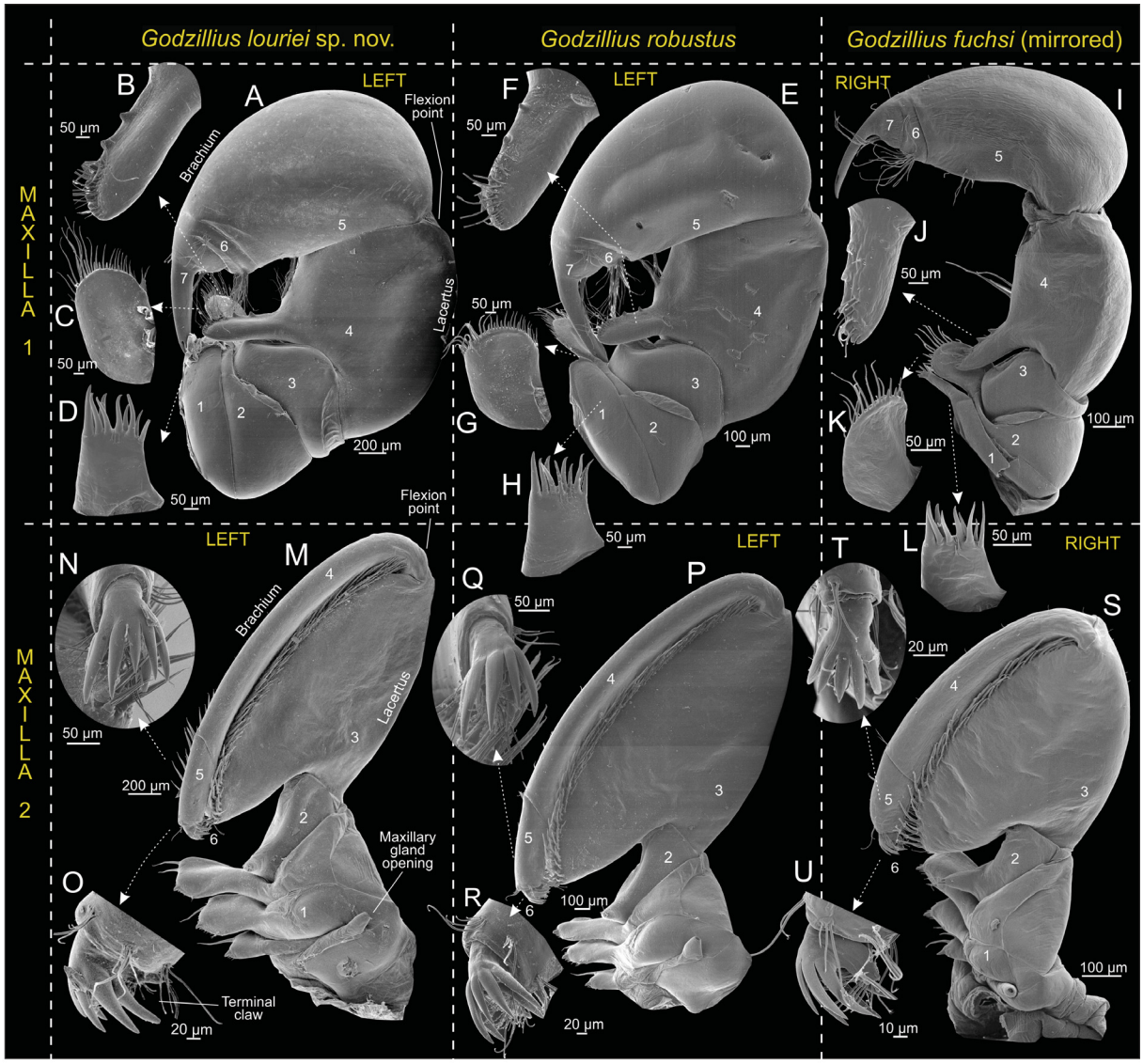


**Fig. 9.** Morphological comparison of maxilla 1 (mx1) and maxilla 2 (mx2) between *Godzillius louriei* sp. nov. (NHMD 669698) (A–D, M–O), *G. robustus* Schram, Yager & Emerson, 1986 (UNSM 1524349) (E–H, P–R) and *G. fuchsi* Gonzalez, Singpiel & Schlagner, 2013 (NHMD 165841) (I–L, S–U), scanning electron microscopy. **A**. Left mx1, posterior face. **B**. Digitiform endite on segment 4, posterior view. **C**. Spatulate endite of segment 2. **D**. Endite of segment 1. **E**. Left mx1, posterior face. **F**. Digitiform endite on segment 4, posterior view. **G**. Spatulate endite of segment 2. **H**. Endite of segment 1. **I**. Right mx1, posterior face (mirrored). **J**. Digitiform endite on segment 4, posterior view. **K**. Spatulate endite of segment 2. **L**. Endite of segment 1. **M**. Left mx2, posterior face. **N**. Apical view of terminal claw. **O**. Posterior view of terminal claw. **P**. Left mx2, posterior face. **Q**. Apical view of terminal claw. **R**. Posterior view of terminal claw. **S**. Left mx2, posterior face. **T**. Apical view of terminal claw. **U**. Posterior view of terminal claw. Small numbers represent segments of mx1 and mx2.

(UFBoot = 100, BPP = 1.0). Similarly, *Godzillius* also formed a fully supported clade (UFBoot = 100; BPP = 1.0), and contained representatives of *G. fuchsi*, *G. louriei* sp. nov. and *G. robustus*, which formed a polytomy.

16S rRNA pairwise distances revealed *Godzillius louriei* sp. nov. has a genetic distance of 15% when compared to all individuals of *G. fuchsi* and *G. robustus* whereas the distance between individuals of *G. fuchsi* and *G. robustus* is 13–14% (Table 3). Within *Godzilliognomus*, the sister genus to *Godzillius* (see Fig. 11), the distance between the two known species, *Godzilliognomus frondosus* and *G. schrami*, is slightly lower at 12–13%.

## Discussion

### Molecular distinction of *Godzillius louriei* sp. nov.

The present study describes a third remipede species of the genus *Godzillius*. Both morphological and molecular approaches provide support for the recovery of *G. louriei* sp. nov. within *Godzillius*, being distinct from the two other species of the genus. There is some indication within the phylogeny that *G. louriei* sp. nov. may be sister to *G. robustus* (Fig. 11); however, further data is needed to clarify

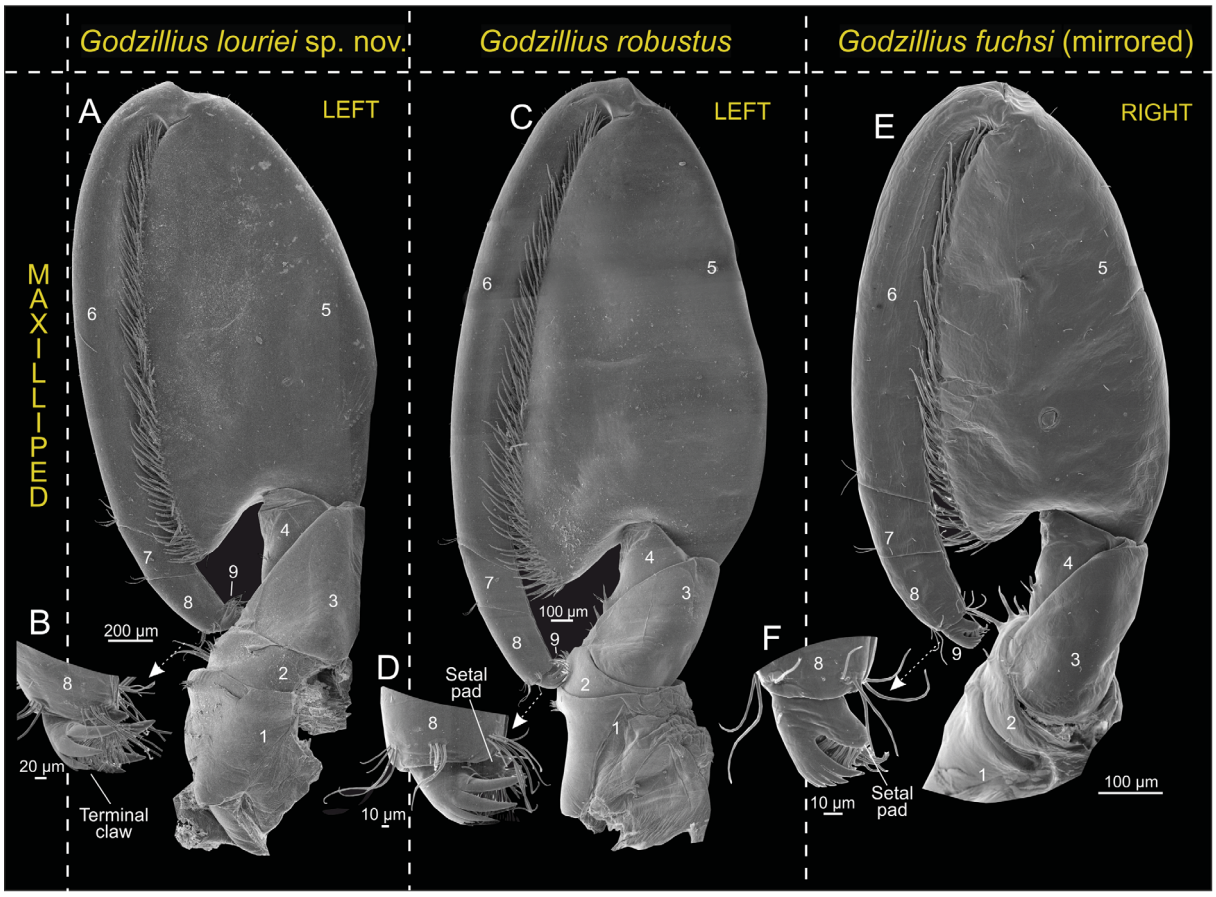


**Fig. 10.** Morphological comparison of maxilliped (mxp) between *Godzillius louriei* sp. nov. (NHMD 669698) (A–B), *G. robustus* Schram, Yager & Emerson, 1986 (UNSM 1524349) (C–D) and *G. fuchsi* Gonzalez, Singpiel & Schlagner, 2013 (NHMD 165841) (E–F), scanning electron microscopy. **A**. Left mxp of *G. louriei* sp. nov., posterior face. **B**. Terminal claw, posterior face. **C**. Left mxp of *G. robustus*, posterior face. **D**. Terminal claw, posterior face. **E**. Right mxp of *G. fuchsi*, posterior face (mirrored). **F**. Terminal claw, posterior face. Small numbers represent segments of mxp.

**Table 2.** Morphological comparison of the species of *Godzillius* Schram, Yager & Emerson, 1986: *G. louriei* sp. nov., *G. robustus* Schram, Yager & Emerson, 2013 and *G. fuchsi* Gonzalez, Singpiel & Schlagner, 1986. All characters denoted with an asterisk (*) are from observations in this study. All other characters are from their respective species descriptions ([1]= Gonzalez *et al*. 2013; [2] = Schram *et al.* 1986).

| | ***G. louriei* sp. nov.** | ***G. robustus*** | ***G. fuchsi*** |
|---|---|---|---|
| **Left mandible, lacinia mobilis, number of denticles** | 5 denticles * | 6 denticles [2] | 5 denticles *<br>5 denticles [1] |
| **Antenna 2, protopod, segment 2** | 1 seta * | 17 setae [2] | 10 setae [1] |
| **Maxilla 1, segment 4, endite, setae and denticles** | 10 denticles, 19–20 setae * | 6–8 denticles, 20–25 setae *<br>6 teeth [2] | 6 denticles, 11–12 setae *<br>not reported [1] |
| **Maxilla 1, segment 1, endite, spines** | 10 large and 3 small spines * | 11 large and 4 small spines *<br>8–9 spines [2] | 10 large and 2 small spines *<br>10 spines [1] |
| **Maxilla 1, segment 2, spatulate endite** | 25–30 setae, 4–5 spines * | 25–30 setae, 5 spines *<br>about 12 moderate to long setae [2] | 15–16 setae, 3–4 spines *<br>22 setae [1] |
| **Maxilla 2, segment 6, terminal claw** | 7 denticles * | 10 denticles [2] | 7 denticles [1] |
| **Maxilliped, segment 9, terminal claw** | reduced setal pad * | reduced setal pad *<br>not reported [2] | protruding setal pad *<br>not reported [1] |

the relationships within *Godzillius*. We compared 16S rRNA pairwise distances within *Godzillius* and found them to be equal to or greater than what is observed within *Godzilliognomus*. In general, the 16S rRNA disparity observed within genera of Remipedia is notably high relative to other crustacean groups (Lefébure *et al*. 2006), which may suggest greater divergence times between remipede species.

**Morphological distinction of *Godzillius louriei* sp. nov.**

The shape of the cephalic shield, articulation of the ventral ramus of antenna 1 and the digitiform maxilla 1 endite fourth segment are key characteristics of the genus *Godzillius* (Schram *et al*. 1986; Gonzalez *et al.* 2013) which are shared by *G. louriei* sp. nov. *Godzillius louriei* sp. nov. can be distinguished from other species of *Godzillius* by several minute morphological characters on the prehensile/raptorial cephalic limbs, maxilla 1, maxilla 2 and maxilliped (Table 2, Figs 9–10). These limbs exhibit notable variation and often harbor specific diagnostic characters, as Koenemann *et al*. (2007) concluded in their detailed morphological phylogeny. The differences between *G. louriei* sp. nov. and its two congeners relate to details such as the number of spines, denticles and setae on the endites of segments 1–3 of maxilla 1, and the number of spines on the terminal claws of maxilla 2 and the maxilliped (see Remarks above and Table 2, Figs 9–10). Based on new SEM examination, we identified several discrepancies between the original descriptions of *G. robustus* (see Schram *et al.* 1986) and *G. fuchsi* (see Gonzalez *et al.* 2013) relative to our newly collected topotypic material, specifically with regards to the spination and setation of maxilla 1 endites (see Table 2). These variations may be due to the use of different microscopy techniques; SEM provides alternative viewpoints of a singular structure at high magnification, capturing spines and setae that may be difficult to view in light microscopy. For instance, neither description of *G. fuchsi* or *G. robustus* report the presence of small proximal spines on the endite of segment 1, nor the presence of spines along the spatulate endite of segment 2 within maxilla 1; yet they are both observed in our SEM analyses. Based on our 16S rRNA data, the material of *G. robustus* is conspecific with similarly named material in GenBank (Fig. 11). A detailed examination of type material is needed to clarify whether the morphological differences are instances of intraspecific variation, or whether the original descriptions lack details in these respects.

**Distribution of the genus *Godzillius* within anchialine habitats**

*Godzillius louriei* sp. nov. marks the first of its genus to be found on the Great Bahama Bank, considerably expanding the known distribution of *Godzillius* throughout the Lucayan Archipelago (Fig 1). The presence of a potential *G. louriei* sp. nov. – *G. robustus* clade is not readily explainable zoogeographically, as the two species occur further from each other (Andros and North Caicos: 700 km) than *G. louriei* sp. nov. and *G. fuchsi* (Andros and Abaco: 135 km) (Fig. 1). All three species are found within the Lucayan Archipelago, but each occurs on separate shallow-water platforms (banks) and are isolated by deep ocean channels. The species of *Godzillius* are only known from their type localities. This may either suggest that they are truly endemic, possibly representing remnants of an earlier broader distribution, or that their distribution spans unexplored or unknown crevicular systems.

While most remipede species have been collected within inland anchialine cave environments (n = 26), a few have been observed in offshore subseafloor marine caves. *Godzillius louriei* sp. nov. marks only the third known remipede species to inhabit subseafloor marine caves, the others being *Xibalbanus cokei* (Yager, 2013), from Caye Chapel Cave, Belize and *Speleonectes kakuki* Daenekas *et al.*, 2009, which also inhabits Conch Sound Blue Hole (Daenekas *et al*. 2009; Yager 2013). Interestingly, *S. kakuki* was collected in the same section of the cave as *G. louriei* sp. nov. (Daenekas *et al*. 2009). Both *X. cokei*

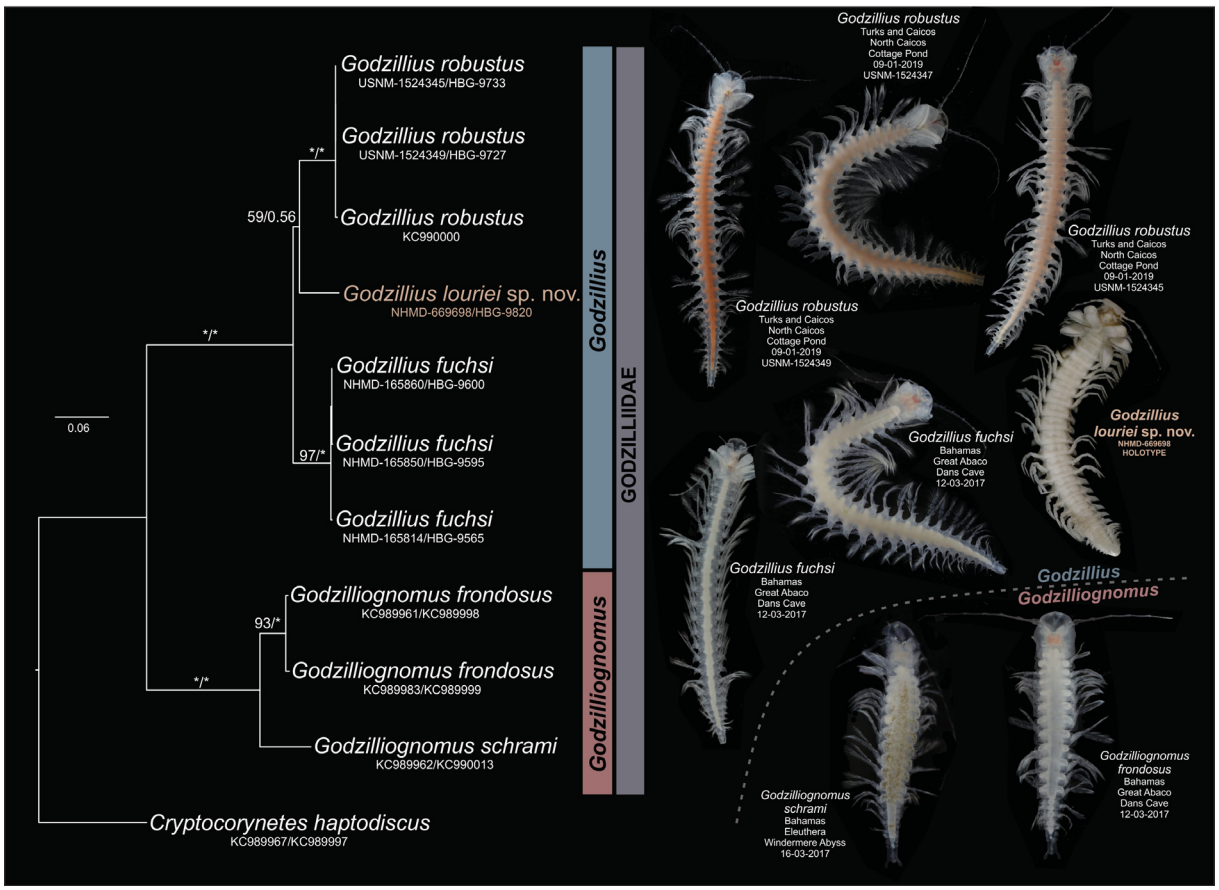


**Fig. 11.** Maximum likelihood analyses and Bayesian Inference of concatenated gene data (16S rRNA and H3) for Godzilliidae. Bootstrap support values and posterior probabilities provided above branches (ML/BI). Any bootstrap value or posterior probability at 100 or 1.0, respectively, is indicated with an asterisk (*). For the concatenated gene analyses, different individuals identified (not this study) as the same species were concatenated together using GenBank sequence data: KC989961+KC989998, KC989983+KC989999 and KC989962+KC990013. Photos of species of Godzilliidae by Jørgen Olesen. All except *Godzillius louriei* sp. nov. are of live specimens. Photos are not to the same scale.

**Table 3.** Pairwise distances comparing 16S rRNA genes across Remipedia (this table is also available as Supplementary File 3).

| | 1 | 2 | 3 | 4 | 5 | 6 | 7 | 8 | 9 | 10 | 11 | 12 | 13 | 14 | 15 | 16 | 17 | 18 | 19 | 20 | 21 | 22 | 23 | 24 | 25 | 26 | 27 | 28 | 29 | 30 | 31 | 32 | 33 | 34 | 35 | 36 | 37 |
|---|---|---|---|---|---|---|---|---|---|---|---|---|---|---|---|---|---|---|---|---|---|---|---|---|---|---|---|---|---|---|---|---|---|---|---|---|---|
| 1. 9565_G_fuchsi | | | | | | | | | | | | | | | | | | | | | | | | | | | | | | | | | | | | | |
| 2. 9600_G_fuchsi | 0.00 | | | | | | | | | | | | | | | | | | | | | | | | | | | | | | | | | | | | |
| 3. 9595_G_fuchsi | 0.00 | 0.00 | | | | | | | | | | | | | | | | | | | | | | | | | | | | | | | | | | | |
| 4. 9727_G_robustus | 0.14 | 0.14 | 0.13 | | | | | | | | | | | | | | | | | | | | | | | | | | | | | | | | | | |
| 5. 9733_G_robustus | 0.14 | 0.14 | 0.13 | 0.00 | | | | | | | | | | | | | | | | | | | | | | | | | | | | | | | | | |
| 6. Godzillius_robustus_03_19_KC990000 | 0.14 | 0.14 | 0.14 | 0.00 | 0.00 | | | | | | | | | | | | | | | | | | | | | | | | | | | | | | | | |
| 7. **9820_G_louriei_n_sp** | **0.15** | **0.15** | **0.15** | **0.15** | **0.15** | **0.15** | | | | | | | | | | | | | | | | | | | | | | | | | | | | | | | |
| 8. Godzilliognomus_frondosus_06_048_4_KC989998 | 0.24 | 0.24 | 0.24 | 0.26 | 0.26 | 0.25 | **0.26** | | | | | | | | | | | | | | | | | | | | | | | | | | | | | | |
| 9. Godzilliognomus_frondosus_AB06_SS_4.1_KC989999 | 0.23 | 0.23 | 0.23 | 0.24 | 0.24 | 0.24 | **0.25** | 0.00 | | | | | | | | | | | | | | | | | | | | | | | | | | | | | |
| 10. Godzilliognomus_schrami_07_048_2_KC990013 | 0.26 | 0.26 | 0.26 | 0.27 | 0.27 | 0.27 | **0.27** | 0.13 | 0.12 | | | | | | | | | | | | | | | | | | | | | | | | | | | | |
| 11. Angirasu_benjamini_06_47_2_KC990007 | 0.29 | 0.29 | 0.29 | 0.31 | 0.31 | 0.31 | **0.30** | 0.29 | 0.27 | 0.29 | | | | | | | | | | | | | | | | | | | | | | | | | | | |
| 12. Angirasu_benjamini_AB06_SS3_KC990011 | 0.29 | 0.29 | 0.29 | 0.30 | 0.30 | 0.31 | **0.30** | 0.29 | 0.27 | 0.29 | 0.01 | | | | | | | | | | | | | | | | | | | | | | | | | | |
| 13. Angirasu_benjamini_AB06_TM1_KC990012 | 0.29 | 0.28 | 0.29 | 0.30 | 0.30 | 0.31 | **0.29** | 0.29 | 0.27 | 0.29 | 0.00 | 0.01 | | | | | | | | | | | | | | | | | | | | | | | | | |
| 14. Cryptocorynetes_elmorei_07_035B_KC989996 | 0.31 | 0.31 | 0.31 | 0.31 | 0.31 | 0.32 | **0.30** | 0.28 | 0.28 | 0.30 | 0.23 | 0.23 | 0.24 | | | | | | | | | | | | | | | | | | | | | | | | |
| 15. Cryptocorynetes_haptodiscus_AB06_SS_1_KC989997 | 0.31 | 0.31 | 0.31 | 0.31 | 0.31 | 0.32 | **0.32** | 0.26 | 0.24 | 0.29 | 0.21 | 0.21 | 0.21 | 0.15 | | | | | | | | | | | | | | | | | | | | | | | |
| 16. Angirasu_parabenjamini_04_023_SK_KC990017 | 0.33 | 0.33 | 0.32 | 0.32 | 0.32 | 0.32 | **0.31** | 0.31 | 0.31 | 0.30 | 0.22 | 0.22 | 0.22 | 0.27 | 0.25 | | | | | | | | | | | | | | | | | | | | | | |
| 17. Kumonga_exleyi_BES_10169_KC990002 | 0.30 | 0.31 | 0.31 | 0.31 | 0.31 | 0.32 | **0.31** | 0.30 | 0.29 | 0.30 | 0.23 | 0.23 | 0.23 | 0.27 | 0.24 | 0.27 | | | | | | | | | | | | | | | | | | | | | |
| 18. Lasionectes_entrichoma_03_16_KC990001 | 0.30 | 0.30 | 0.30 | 0.33 | 0.33 | 0.33 | **0.30** | 0.34 | 0.33 | 0.33 | 0.25 | 0.25 | 0.25 | 0.26 | 0.25 | 0.25 | 0.28 | | | | | | | | | | | | | | | | | | | | |
| 19. Micropacter_yagerae_41698_KC990003 | 0.31 | 0.31 | 0.31 | 0.30 | 0.30 | 0.31 | **0.30** | 0.33 | 0.32 | 0.34 | 0.25 | 0.25 | 0.25 | 0.31 | 0.28 | 0.27 | 0.26 | 0.22 | | | | | | | | | | | | | | | | | | | |
| 20. Speleonectes_kakuki_BH330_KC990009 | 0.31 | 0.31 | 0.31 | 0.30 | 0.30 | 0.31 | **0.30** | 0.33 | 0.32 | 0.34 | 0.25 | 0.25 | 0.25 | 0.31 | 0.28 | 0.27 | 0.26 | 0.22 | 0.00 | | | | | | | | | | | | | | | | | | |
| 21. Speleonectes_lucayensis_AB06_LR_1_KC990010 | 0.29 | 0.29 | 0.30 | 0.31 | 0.31 | 0.32 | **0.31** | 0.31 | 0.30 | 0.32 | 0.23 | 0.23 | 0.23 | 0.28 | 0.27 | 0.27 | 0.25 | 0.20 | 0.17 | 0.17 | | | | | | | | | | | | | | | | | |
| 22. Pleomothra_apletocheles_AB06_RS2_KC990004 | 0.30 | 0.30 | 0.30 | 0.31 | 0.31 | 0.31 | **0.30** | 0.33 | 0.32 | 0.35 | 0.27 | 0.27 | 0.27 | 0.30 | 0.28 | 0.31 | 0.28 | 0.25 | 0.24 | 0.24 | 0.24 | | | | | | | | | | | | | | | | |
| 23. Pleomothra_apletocheles_AB06_SS2_KC990005 | 0.30 | 0.30 | 0.30 | 0.31 | 0.31 | 0.31 | **0.30** | 0.33 | 0.32 | 0.35 | 0.27 | 0.27 | 0.27 | 0.30 | 0.28 | 0.31 | 0.28 | 0.25 | 0.24 | 0.24 | 0.24 | 0.00 | | | | | | | | | | | | | | | |
| 24. Pleomothra_apletocheles_GU067680 | 0.29 | 0.29 | 0.29 | 0.30 | 0.30 | 0.30 | **0.29** | 0.32 | 0.32 | 0.34 | 0.27 | 0.27 | 0.27 | 0.30 | 0.28 | 0.31 | 0.28 | 0.25 | 0.25 | 0.25 | 0.25 | 0.00 | 0.00 | | | | | | | | | | | | | | |
| 25. Pleomothra_nov_sp_07_038_KC990014 | 0.30 | 0.30 | 0.30 | 0.29 | 0.29 | 0.29 | **0.29** | 0.32 | 0.32 | 0.33 | 0.25 | 0.25 | 0.25 | 0.29 | 0.26 | 0.27 | 0.28 | 0.23 | 0.23 | 0.23 | 0.23 | 0.14 | 0.14 | 0.14 | | | | | | | | | | | | | |
| 26. Morlockia_atlantida_DZUL_9999_GBIF_FJ905031 | 0.30 | 0.30 | 0.30 | 0.30 | 0.30 | 0.30 | **0.30** | 0.30 | 0.30 | 0.30 | 0.23 | 0.23 | 0.23 | 0.29 | 0.26 | 0.27 | 0.27 | 0.24 | 0.26 | 0.26 | 0.25 | 0.30 | 0.30 | 0.30 | 0.25 | | | | | | | | | | | |
| 27. Morlockia_atlantida_LZ_1_1_FJ905032 | 0.30 | 0.30 | 0.30 | 0.30 | 0.30 | 0.30 | **0.31** | 0.30 | 0.30 | 0.30 | 0.23 | 0.23 | 0.23 | 0.29 | 0.26 | 0.27 | 0.27 | 0.24 | 0.26 | 0.26 | 0.25 | 0.30 | 0.30 | 0.30 | 0.25 | 0.00 | | | | | | | | | | |
| 28. Morlockia_atlantida_LZ_2_1_FJ905033 | 0.30 | 0.30 | 0.30 | 0.30 | 0.30 | 0.30 | **0.31** | 0.29 | 0.29 | 0.30 | 0.23 | 0.23 | 0.23 | 0.29 | 0.26 | 0.27 | 0.27 | 0.24 | 0.26 | 0.26 | 0.25 | 0.30 | 0.30 | 0.30 | 0.25 | 0.00 | 0.00 | | | | | | | | | |
| 29. Morlockia_atlantida_LZ_2_3_FJ905034 | 0.30 | 0.30 | 0.30 | 0.30 | 0.30 | 0.30 | **0.30** | 0.30 | 0.30 | 0.30 | 0.23 | 0.23 | 0.23 | 0.29 | 0.26 | 0.27 | 0.27 | 0.24 | 0.26 | 0.26 | 0.25 | 0.30 | 0.30 | 0.30 | 0.25 | 0.00 | 0.00 | 0.00 | | | | | | | | |
| 30. Morlockia_ondinae_LZ_1_2_FJ905035 | 0.27 | 0.27 | 0.27 | 0.31 | 0.31 | 0.31 | **0.30** | 0.28 | 0.28 | 0.28 | 0.23 | 0.23 | 0.23 | 0.30 | 0.26 | 0.26 | 0.27 | 0.24 | 0.27 | 0.27 | 0.25 | 0.29 | 0.29 | 0.29 | 0.25 | 0.12 | 0.12 | 0.12 | 0.12 | | | | | | | |
| 31. Morlockia_emersoni_05_22_1_KC990008 | 0.28 | 0.29 | 0.28 | 0.29 | 0.29 | 0.29 | **0.30** | 0.28 | 0.28 | 0.27 | 0.25 | 0.26 | 0.25 | 0.29 | 0.28 | 0.25 | 0.27 | 0.24 | 0.25 | 0.25 | 0.25 | 0.29 | 0.29 | 0.28 | 0.27 | 0.20 | 0.20 | 0.20 | 0.20 | 0.19 | | | | | | |
| 32. Morlockia_williamsi_08_033_4_KC990018 | 0.30 | 0.30 | 0.30 | 0.31 | 0.31 | 0.31 | **0.30** | 0.31 | 0.30 | 0.33 | 0.26 | 0.26 | 0.26 | 0.30 | 0.25 | 0.28 | 0.27 | 0.24 | 0.26 | 0.26 | 0.23 | 0.27 | 0.27 | 0.27 | 0.24 | 0.21 | 0.21 | 0.20 | 0.21 | 0.20 | 0.21 | | | | | |
| 33. Speleonectes_nov_sp_AB06_047_6_KC990015 | 0.28 | 0.28 | 0.28 | 0.28 | 0.28 | 0.28 | **0.30** | 0.27 | 0.27 | 0.29 | 0.25 | 0.25 | 0.25 | 0.28 | 0.28 | 0.26 | 0.28 | 0.26 | 0.22 | 0.22 | 0.22 | 0.26 | 0.26 | 0.27 | 0.25 | 0.29 | 0.29 | 0.29 | 0.29 | 0.27 | 0.24 | 0.27 | | | | |
| 34. Speleonectes_nov_sp_AB06_DC_1.1_KC990016 | 0.28 | 0.27 | 0.27 | 0.27 | 0.27 | 0.28 | **0.30** | 0.29 | 0.27 | 0.31 | 0.25 | 0.26 | 0.25 | 0.28 | 0.27 | 0.28 | 0.26 | 0.26 | 0.23 | 0.23 | 0.23 | 0.25 | 0.25 | 0.26 | 0.25 | 0.28 | 0.29 | 0.29 | 0.28 | 0.27 | 0.25 | 0.27 | 0.02 | | | |
| 35. Xibalabanus_cf_tulumensis_06_41H_KC990019 | 0.35 | 0.35 | 0.35 | 0.34 | 0.34 | 0.34 | **0.35** | 0.33 | 0.33 | 0.32 | 0.29 | 0.29 | 0.29 | 0.30 | 0.31 | 0.28 | 0.29 | 0.29 | 0.28 | 0.28 | 0.30 | 0.32 | 0.32 | 0.33 | 0.30 | 0.28 | 0.28 | 0.28 | 0.28 | 0.27 | 0.28 | 0.31 | 0.28 | 0.29 | | |
| 36. Xibalbanus_tulumensis_AY456190 | 0.34 | 0.34 | 0.35 | 0.34 | 0.34 | 0.35 | **0.35** | 0.34 | 0.32 | 0.32 | 0.29 | 0.29 | 0.28 | 0.29 | 0.30 | 0.28 | 0.28 | 0.28 | 0.27 | 0.27 | 0.28 | 0.31 | 0.31 | 0.31 | 0.29 | 0.26 | 0.26 | 0.26 | 0.26 | 0.26 | 0.26 | 0.28 | 0.28 | 0.28 | 0.01 | |
| 37. Xibalbanus_cozumelensis_ZMUC_CRU_4793_KX830886 | 0.36 | 0.36 | 0.36 | 0.34 | 0.34 | 0.35 | **0.35** | 0.33 | 0.31 | 0.33 | 0.31 | 0.31 | 0.30 | 0.31 | 0.32 | 0.29 | 0.29 | 0.30 | 0.29 | 0.29 | 0.29 | 0.31 | 0.31 | 0.30 | 0.27 | 0.28 | 0.28 | 0.28 | 0.28 | 0.27 | 0.27 | 0.29 | 0.27 | 0.28 | 0.17 | 0.13 |
| 38. Speleonectes_gironensis_AF370874 | 0.37 | 0.37 | 0.37 | 0.39 | 0.39 | 0.40 | **0.40** | 0.37 | 0.36 | 0.37 | 0.33 | 0.33 | 0.33 | 0.37 | 0.36 | 0.33 | 0.36 | 0.34 | 0.36 | 0.36 | 0.35 | 0.34 | 0.34 | 0.34 | 0.33 | 0.31 | 0.31 | 0.31 | 0.31 | 0.29 | 0.30 | 0.33 | 0.34 | 0.34 | 0.34 | 0.33 | 0.36 |

and *G. louriei* sp. nov. are only known from their type localities, whereas *S. kakuki* has been observed within both inland anchialine cave systems and subseafloor marine caves (Daenekas *et al*. 2009; Yager 2013). The summarized occurrence of remipedes in both types of cave systems, with one species (*S. kakuki*) spanning both, suggests that a close relationship between these habitats exists, either currently or historically. van Hengstum *et al*. (2019) proposed that anchialine and marine caves may be linked through allogenic succession and should be considered parts of the "anchialine habitat continuum".

The idea of a continuous or crevicular "spelean corridor" has been shown as a means for anchialine fauna to disperse throughout subterranean systems (Hart *et al*. 1985; Hunter *et al.* 2008; Gonzalez *et al*. 2017). Historic sea level fluctuation may also have contributed to the present day distribution of *Godzillius*. Anchialine habitats are shown to shift with sea level change, resulting in different community compositions within cave environments (van Hengstum *et al*. 2019). The type localities of *G. louriei* sp. nov., *G. fuchsi* and *G. robustus* (Conch Sound, Dan's Cave, Ralph's Sink, Cottage Pond) all contain large speleothems within their passages, which only form in air by dripping water (BG, BK, TI, pers. obs.; Koenemann *et al.* 2004; Surić *et al*. 2005), indicating that the caves were dry during glacial periods of low sea level. Because of these historic complexities, caution must be applied when assessing anchialine fauna distribution patterns, as we are likely only seeing a snapshot of a dynamic transgression and regression of anchialine habitats along karstic coastlines.

## Acknowledgements

Field work was supported by the Bahamas Cave Research Foundation (to BK, KB, TI) for the Andros expedition which resulted in the collection of the new remipede species; Abaco (Bahamas) collecting was partly funded by the Schander Memorial Fund (to KM) and the Carlsberg Foundation (to JO); Turks and Caicos collecting was funded by the Smithsonian Global Genome Initiative – Rolling Awards Program (GGI-2019-Rolling-214 to KJO) and by the Peter Buck Fellowship Program (to BCG). Many thanks to the Bahamas Department of Marine Resources for the research permit. Special thanks to the Turks and Caicos Islands Department of Environment and Coastal Resources (DECR) – Ministry of Tourism, Environment, Heritage, Culture & Gaming for their willingness to grant collection and export permits to our team. This material is based upon work supported by the National Science Foundation Graduate Research Fellowship Program under Grant No. (M1703014). In addition, many thanks to the Cave Conservancy Foundation for providing funding support for LB. This is contribution #248 from the Division of Coastlines and Oceans in the Institute of Environment at Florida International University. Last, but certainly not least, we wish to express our appreciation to Stefan Koenemann for his extensive and important work on Remipedia.

## References

Altschul S.F., Gish W., Miller W., Myers E.W. & Lipman D.J. 1990. Basic local alignment search tool. *Journal of Molecular Biology* 215: 403–410. https://doi.org/10.1016/S0022-2836(05)80360-2

Benson D.A., Boguski M.S., Lipman D.J., Ostell J. & Ouellette B.F.F. 1998. GenBank. *Nucleic Acids Research* 26: 1–7. https://doi.org/10.1093/nar/26.1.1

Bishop R.E., Humphreys W.F., Cukrov N., Žic V., Boxshall G.A., Cukrov M., Iliffe T.M., Kršinić F., Moore W.S., Pohlman J.W. & Sket B. 2015. 'Anchialine' redefined as a subterranean estuary in a crevicular or cavernous geological setting. *Journal of Crustacean Biology* 35: 511–514. https://doi.org/10.1163/1937240X-00002335

Brankovits D., Pohlman J.W., Niemann H., Leigh M.B., Leewis M.C., Becker K.W., Iliffe T.M., Alvarez F., Lehmann M.F. & Phillips B. 2017. Methane- and dissolved organic carbon-fueled microbial loop supports a tropical subterranean estuary ecosystem. *Nature Communications* 8: 1–12. https://doi.org/10.1038/s41467-017-01776-x

Cánovas F., Jurado-Rivera J.A., Cerro-Gálvez E., Juan C., Jaume D. & Pons J. 2016. DNA barcodes, cryptic diversity and phylogeography of a W Mediterranean assemblage of thermosbaenacean crustaceans. *Zoologica Scripta* 45: 659–670. https://doi.org/10.1111/zsc.12173

Colgan D.J., McLauchlan A., Wilson G.D.F., Livingston S.P., Edgecombe G.D., Macaranas J., Cassis G. & Gray M.R. 1998. Histone H3 and U2 snRNA DNA sequences and arthropod molecular evolution. *Australian Journal of Zoology* 46: 419–437. https://doi.org/10.1071/ZO98048

Daenekas J., Iliffe T.M., Yager J. & Koenemann S. 2009. *Speleonectes kakuki*, a new species of Remipedia (Crustacea) from anchialine and sub-seafloor caves on Andros and Cat Island, Bahamas. *Zootaxa* 2016 (1): 51–66. https://doi.org/10.11646/zootaxa.2016.1.3

Darriba D., Taboada G.L., Doallo R. & Posada D. 2012. jModelTest 2: more models, new heuristics and parallel computing. *Nature Methods* 9: e772. https://doi.org/10.1038/nmeth.2109

Farr M. 2017. *The Darkness Beckons: The History and Development of World Cave Diving.* Vertebrate Publishing.

Farr M. & Palmer R. 1984. The blue holes: description and structure. *In:* Ford T.D. (ed.) *Bahamas Blue Holes 1981–1982*. *Cave Science* 11 (1): 9–22.

Gonzalez B.C., Singpiel A. & Schlagner P. 2013. *Godzillius fuchsi*, a new species of Remipedia (Godzilliidae) from Abaco Island, Bahamas. *Journal of Crustacean Biology* 33: 275–285. https://doi.org/10.1163/1937240X-00002132

Gonzalez B.C., Martínez A., Borda E., Iliffe T.M., Fontaneto D. & Worsaae K. 2017. Genetic spatial structure of an anchialine cave annelid indicates connectivity within – but not between – islands of the Great Bahama Bank. *Molecular Phylogenetics and Evolution* 109: 259–270. https://doi.org/10.1016/j.ympev.2017.01.003

Guindon S. & Gascuel O. 2003. A simple, fast, and accurate method to estimate large phylogenies by maximum likelihood. *Systematic Biology* 52: 696–704. https://doi.org/10.1080/10635150390235520

Hart C.W. Jr, Manning R.B. & Iliffe T.M. 1985. The fauna of Atlantic marine caves: evidence of dispersal by sea floor spreading while maintaining ties to deep waters. *Proceedings of the Biological Society of Washington* 98: 288–292.

Hoang D.T., Chernomor O., von Haeseler A., Minh B.Q. & Vinh L.S. 2018. UFBoot2: improving the ultrafast bootstrap approximation. *Molecular Biology and Evolution* 35: 518–522. https://doi.org/10.1093/molbev/msx281

Hoenemann M., Neiber M.T., Humphreys W.F., Iliffe T.M., Li D., Schram F.R. & Koenemann S. 2013. Phylogenetic analysis and systematic revision of Remipedia (Nectiopoda) from Bayesian analysis of molecular data. *Journal of Crustacean Biology* 33: 603–619. https://doi.org/10.1163/1937240X-00002179

Hunter R.L., Webb M.S., Iliffe T.M. & Alvarado Bremer J.R. 2008. Phylogeny and historical biogeography of the cave-adapted shrimp genus *Typhlatya* (Atyidae) in the Caribbean Sea and western Atlantic. *Journal of Biogeography* 35: 65–75. https://doi.org/10.1111/j.1365-2699.2007.01767.x

Juan C., Guzik M.T., Jaume D. & Cooper S.J.B. 2010. Evolution in caves: Darwin's 'wrecks of ancient life' in the molecular era. *Molecular Ecology* 19: 3865–3880. https://doi.org/10.1111/j.1365-294X.2010.04759.x

Kalyaanamoorthy S., Minh B.Q., Wong T.K.F., von Haeseler A. & Jermiin L.S. 2017. ModelFinder: fast model selection for accurate phylogenetic estimates. *Nature Methods* 14: 587–589. https://doi.org/10.1038/nmeth.4285

Katoh K., Rozewicki J. & Yamada K.D. 2019. MAFFT online service: multiple sequence alignment, interactive sequence choice and visualization. *Briefings in Bioinformatics* 20: 1160–1166. https://doi.org/10.1093/bib/bbx108

Kearse M., Moir R., Wilson A., Stones-Havas S., Cheung M., Sturrock S., Buxton S., Cooper A., Markowitz S., Duran C., Thierer T., Ashton B., Meintjes P. & Drummond A. 2012. Geneious Basic: an integrated and extendable desktop software platform for the organization and analysis of sequence data. *Bioinformatics* 28: 1647–1649. https://doi.org/10.1093/bioinformatics/bts199

Koenemann S. & Iliffe T.M. 2014. Class Remipedia Yager, 1981. *In*: Klein V.K. (ed.) *Treatise on Zoology-Anatomy, Taxonomy, Biology. The Crustacea. Volume 4, part A*: 125–177. Brill, Leiden.

Koenemann S., Iliffe T.M. & Yager J. 2004. *Kaloketos pilosus,* a new genus and species of Remipedia (Crustacea) from the Turks and Caicos Islands. *Zootaxa* 618 (1): 1–12. https://doi.org/10.11646/zootaxa.618.1.1

Koenemann S., Schram F.R., Hönemann M. & Iliffe T.M. 2007. Phylogenetic analysis of Remipedia (Crustacea). *Organisms Diversity & Evolution* 7: 33–51. https://doi.org/10.1016/j.ode.2006.07.001

Kumar S., Stecher G. & Tamura K. 2016. MEGA7: Molecular evolutionary genetics analysis version 7.0 for bigger datasets. *Molecular Biology and Evolution* 33: 1870–1874. https://doi.org/10.1093/molbev/msw054

Lefébure T., Douady C.J., Gouy M. & Gibert J. 2006. Relationship between morphological taxonomy and molecular divergence within Crustacea: proposal of a molecular threshold to help species delimitation. *Molecular Phylogenetics and Evolution* 40: 435–447. https://doi.org/10.1016/j.ympev.2006.03.014

Miller M.A., Pfeiffer W. & Schwartz T. 2010. "Creating the CIPRES Science Gateway for inference of large phylogenetic trees." *In*: *Proceedings of the Gateway Computing Environments Workshop (GCE)*: 1–8. IEEE Xplore, New Orleans. https://doi.org/10.1109/GCE.2010.5676129

Mylroie J.E. & Carew J.L. 1990. The flank margin model for dissolution cave development in carbonate platforms. *Earth Surface Processes and Landforms* 15: 413–424. https://doi.org/10.1002/esp.3290150505

Mylroie J.E. & Mylroie J.R. 2011. Void development on carbonate coasts: creation of anchialine habitats. *Hydrobiologia* 677: 15–32. https://doi.org/10.1007/s10750-010-0542-y

Natural Earth 2020. Natural Earth. Free vector and raster map data at 1:10m, 1:50m, and 1:100m scales. Available from https://naturalearthdata.com [accessed 18 May 2021].

Neiber M.T., Hansen F.C., Iliffe T.M., Gonzalez B.C. & Koenemann S. 2012. Molecular taxonomy of *Speleonectes fuchscockburni*, a new pseudocryptic species of Remipedia (Crustacea) from an anchialine cave system on the Yucatán Peninsula, Quintana Roo, Mexico. *Zootaxa* 3190 (1): 31–46. https://doi.org/10.11646/zootaxa.3190.1.2

Nguyen L.T., Schmidt H.A., von Haeseler A. & Minh B.Q. 2014. IQ-TREE: A fast and effective stochastic algorithm for estimating maximum-likelihood phylogenies. *Molecular Biology and Evolution* 32: 268–274. https://doi.org/10.1093/molbev/msu300

Olesen J., Meland K., Glenner H., van Hengstum P.J. & Iliffe T.M. 2017. *Xibalbanus cozumelensis*, a new species of Remipedia (Crustacea) from Cozumel, Mexico, and a molecular phylogeny of *Xibalbanus* on the Yucatán Peninsula. *European Journal of Taxonomy* 316: 1–27. https://doi.org/10.5852/ejt.2017.316

QGIS Development Team 2020. QGIS Geographic Information System, ver. 3.12. Open Source Geospatial Foundation. Available from https://qgis.org [accessed 19 Mar. 2021].

Pais F.S.M., Ruy P.C., Oliveira G. & Coimbra R.S. 2014. Assessing the efficiency of multiple sequence alignment programs. *Algorithms for Molecular Biology* 9: 1–8. https://doi.org/10.1186/1748-7188-9-4

Palmer R. 1997. *Deep into Blue Holes*. Media Publishing, Nassau, Bahamas.

Palumbi S., Martin A., Romano S., McMillan W.O., Stice L. & Grabowski G. 2002. *The Simple Fool's Guide to PCR*. Ver. 2. Department of Zoology and Kewalo Marine Laboratory, Honolulu.

Rambaut A., Drummond A.J., Xie D., Baele G. & Suchard M.A. 2018. Posterior summarization in Bayesian phylogenetics using Tracer 1.7. *Systematic Biology* 67: 901–904. https://doi.org/10.1093/sysbio/syy032

Reid W.V. 1998. Biodiversity hotspots. *Trends in Ecology & Evolution* 13: 275–280. https://doi.org/10.1016/S0169-5347(98)01363-9

Ronquist F., Teslenko M., van der Mark P., Ayres D.L., Darling A., Höhna S., Larget B., Liu L., Suchard M.A. & Huelsenbeck J.P. 2012. MrBayes 3.2: Efficient Bayesian phylogenetic inference and model choice across a large model space. *Systematic Biology* 61: 539–542. https://doi.org/10.1093/sysbio/sys029

Schram F.R., Yager J. & Emerson M.J. 1986. Remipedia Part 1. Systematics. *San Diego Society of Natural History, Memoir* 15: 1–60.

Song H., Buhay J.E., Whiting M.F. & Crandall K.A. 2008. Many species in one: DNA barcoding overestimates the number of species when nuclear mitochondrial pseudogenes are coamplified. *Proceedings of the National Academy of Sciences* 105: 13486–13491. https://doi.org/10.1073/pnas.0803076105

Surić M., Juračić M., Horvatinčić N. & Bronić I.K. 2005. Late Pleistocene–Holocene sea-level rise and the pattern of coastal karst inundation: records from submerged speleothems along the Eastern Adriatic Coast (Croatia). *Marine Geology* 214: 163–175. https://doi.org/10.1016/j.margeo.2004.10.030

van Hengstum P.J., Cresswell J.N., Milne G.A. & Iliffe T.M. 2019. Development of anchialine cave habitats and karst subterranean estuaries since the last ice age. *Scientific Reports* 9: 1–10. https://doi.org/10.1038/s41598-019-48058-8

Yager J. 2013. *Speleonectes cokei*, new species of Remipedia (Crustacea: Speleonectidae) from a submerged ocean cave near Caye Chapel, Belize. *Zootaxa* 3710 (4): 354–362. https://doi.org/10.11646/zootaxa.3710.4.4

Zhou X., Shen X.X., Hittinger C.T. & Rokas A. 2017. Evaluating fast Maximum Likelihood-based phylogenetic programs using empirical phylogenomic data sets. *Molecular Biology and Evolution* 35: 486–503. https://doi.org/10.1093/molbev/msx302

*Manuscript received: 1 December 2020*
*Manuscript accepted: 13 April 2021*
*Published on: 7 June 2021*
*Topic editor: Rudy Jocqué*
*Desk editor: Danny Eibye-Jacobsen*

Sciences, Brussels, Belgium; Natural History Museum of Denmark, Copenhagen, Denmark; Naturalis Biodiversity Center, Leiden, the Netherlands; Museo Nacional de Ciencias Naturales-CSIC, Madrid, Spain; Real Jardín Botánico de Madrid CSIC, Spain; Zoological Research Museum Alexander Koenig, Bonn, Germany; National Museum, Prague, Czech Republic.

**Supplemental File 1.**
Maximum likelihood analyses of 16S rRNA for Godzilliidae. Bootstrap support values provided above branches.
https://doi.org/10.5852/ejt.2021.751.1383.4351

**Supplemental File 2.**
Maximum likelihood analyses of H3 for Godzilliidae. Bootstrap support values provided above branches.
https://doi.org/10.5852/ejt.2021.751.1383.4353

**Supplemental File 3.**
Pairwise distances comparing 16S rRNA genes across Remipedia (identical to Table 3 in text above).
https://doi.org/10.5852/ejt.2021.751.1383.4355